Pulmonary ventilation and perfusion assessed by electrical impedance tomography

Experimental studies in pigs

Anneli Fagerberg

Department of Anaesthesiology and Intensive Care
Institute of Clinical Sciences at Sahlgrenska Academy
University of Gothenburg
Gothenburg, Sweden
2009

ISBN 978-91-628-7853-5
http://hdl.handle.net/2077/20462

Printed by Intellecta Infolog AB
Gothenburg, Sweden 2009

ABSTRACT

Pulmonary ventilation and perfusion and ventilation/perfusion (V/Q) matching determine gas exchange in every lung unit in the healthy state and in the pathologically altered lung. Mismatch of V and Q lead to hypoxaemia and hypercapnia and monitoring of V/Q relations are thus important in critical illness.

This thesis focuses on electrical impedance tomography (EIT) to monitor pulmonary perfusion and its relation to ventilation in physiological conditions and in endotoxinaemic acute lung injury (ALI) in a porcine experimental model.
EIT is a non-invasive, non-radiant continuous monitoring technique generating images of impedance distribution changes within the thorax. Blood and air differ considerably in impedance properties, resulting in characteristic distribution images of pulmonary ventilation and perfusion respectively.
The methodology of assessing global perfusion by EIT was evaluated in the healthy state during interventions resembling acute hypovolaemia and recruitment manoeuvres. The pulse synchronous amplitude of systolic impedance change, measured during apnoea, correlated to a wide range of stroke volumes measured by the pulmonary artery catheter, as an estimate of pulmonary perfusion.
The methodology was expanded to include regional perfusion and its relation to ventilation by combined measurements during apnoea and ventilation, generating estimates of V/Q relations. Global EIT measurements correlated significantly to venous admixture and alveolar dead space calculated by standard methods. Regional EIT measurements of V and Q provided physiologically relevant results under dynamic conditions.
The monitoring technique was applied in pigs subjected to endotoxinaemic ALI to assess changes in regional V and Q and V/Q matching. V/Q mismatch developed primarily as a result of dorsal redistribution and increased heterogeneity of perfusion.
Finally, pre-treatment with the angiotensin converting enzyme (ACE) inhibitor enalapril to reduce angiotensin II levels and attenuate the inflammation and V/Q mismatch in endotoxinaemic ALI was examined, employing EIT monitoring. The investigation failed to provide support for the hypothesis that ACE inhibition could improve V/Q mismatch and thus gas exchange.

In conclusion, this thesis demonstrated that the EIT technique could be used to assess global and regional pulmonary perfusion and its relation to ventilation in physiological as well as pathological conditions

Key words: electrical impedance tomography, pig, V/Q matching, endotoxinaemic ALI, ACE inhibitor

CONTENTS

LIST OF PAPERS

This thesis is based on the following papers which will be referred to in the text by their Roman numerals I - IV.

I Fagerberg A, Stenqvist O, Åneman A. Monitoring pulmonary perfusion by electrical impedance tomography: an evaluation in a pig model
Acta Anaesthesiol Scand. 2009, 53(2):152-8

II Fagerberg A, Stenqvist O, Åneman A. Electrical impedance tomography applied to assess matching of pulmonary ventilation and perfusion in a porcine experimental model
Critical Care 2009, 13(2):R34

III Fagerberg A, Søndergaard S, Karason S, Åneman A.
Electrical impedance tomography can be used to assess heterogeneity of pulmonary ventilation and perfusion during acute lung injury in pigs
Accepted Acta Anaesthesiol Scand.

IV Fagerberg A, Søndergaard S, Casselbrant A, Åneman A.
Angiotensin-converting enzyme inhibition during endotoxinaemic acute lung injury in pigs does not affect ventilation/perfusion changes monitored by electrical impedance tomography
Submitted

ABBREVIATIONS

ACE	angiotensin-converting enzyme
ALI	acute lung injury
Ang II	angiotensin II
ANOVA	analysis of variance
AP	arterial pressure
ARDS	acute respiratory distress syndrome
AT_1	Ang II type 1 receptor
AT_2	Ang II type 2 receptor
AU	arbitrary unit
AUC_Z	area under the impedance curve
B_{infl}	balloon inflation
BL	baseline
CO	cardiac output
CTRL	control
EIT	electrical impedance tomography
ENAL	enalapril-treated animal
ETX	endotoxin
FRC	functional residual capacity
HR	heart rate
ICU	intensive care unit
I/D	insertion/deletion
MAP	mean arterial pressure
MIGET	multiple inert gas elimination technique
MPAP	mean pulmonary artery pressure
MLR	multiple linear regression
MRI	magnetic resonance imaging
OD	optical density
PAC	pulmonary artery catheter
P_{aw}	airway pressure
PEEP	positive end-expiratory pressure
PET	positron emission tomography
PIM	pulmonary intravascular macrophage
P_{oes}	oesophageal pressure
P_{plat}	plateau pressure in ventilator
P_{tp}	transpulmonary pressure
P_{tr}	tracheal pressure
PVR	pulmonary vascular resistance
Q	perfusion
Q_s/Q_t	pulmonary shunt fraction
R	resistance

RAS	renin-angiotensin system
ROI	region of interest
SD	standard deviation
SV	stroke volume
S_vO_2	mixed venous oxygen saturation
SVR	systemic vascular resistance
TV	tidal volume
V	ventilation
VDC	volume dependent compliance
VDC_{low}	VDC at the low volume part of the tidal breath
VDC_{mid}	VDC at the middle volume part of the tidal breath
VDC_{high}	VDC at the high volume part of the tidal breath
V_D/V_T	pulmonary dead space fraction
X	reactance
Z	impedance
ΔZ_{sys}	change in systolic impedance amplitude
Z_V	ventilation-induced change in thoracic impedance
Z_Q	perfusion-induced change in thoracic impedance

Questions	Methods	Results	Conclusions
Can EIT assess pulmonary perfusion?	Comparison of pulse synchronous impedance amplitudes by EIT with stroke volumes (SV) determined by the pulmonary artery catheter (PAC) in healthy pigs	Pulmonary perfusion measured by EIT correlated significantly to SV determined by the PAC, with a bias of -7% and 95% limits of agreements of -51 to 36% to detect relative changes	EIT provided relevant assessments of pulmonary perfusion for a wide range of SV
Can EIT assess *regional* pulmonary perfusion and ventilation/perfusion (V/Q) matching? Does global EIT V/Q relations correlate to venous admixture and dead space?	Regional perfusion and combined EIT measurements of V and Q within four regions of interest (ROIs) Correlating V/Q with standard calculations of venous admixture and dead space	Regional differences in pulmonary perfusion and V/Q matching could be determined by EIT and global V/Q correlated to venous admixture and dead space	EIT could assess regional distribution of pulmonary perfusion and ventilation with globally relevant estimates of venous admixture and dead space
Is EIT relevant in determining V/Q matching in endotoxinaemic ALI?	Regional perfusion and combined EIT measurements of V and Q within four regions of interest (ROIs) in endotoxinaemic pigs Correlating V/Q with standard calculations of venous admixture and dead space	EIT determined redistribution of V and Q and heterogeneity of in particular Q. Global V/Q relations during endotoxinaemia correlated to venous admixture and dead space	EIT highlighted regional redistribution and mismatch of V and Q in a common experimental model of ALI
Can an anti-inflammatory strategy based on enalapril improve V/Q matching in endotoxinaemic ALI?	Enalapril pre-treated animals were compared to controls for up to 150 minutes of endotoxinaemic ALI	No differences were observed by EIT between enalapril treated and control animals in V/Q distribution and matching and gas exchange	Enalapril does not attenuate V/Q mismatch and impaired gas exchange in endotoxinaemic ALI

INTRODUCTION

Mismatch of pulmonary perfusion and ventilation is common and fundamentally important in the pathology of hypoxaemia and hypercapnia in critically ill patients. Infection is a leading cause of respiratory failure requiring admission to the intensive care unit (ICU). The complex haemodynamic alterations associated with infectious processes are manifested in the pulmonary vasculature by for example hyperdynamic blood flow, formation of capillary microthrombi, increased permeability and a number of other processes. However, increased heterogeneity of pulmonary perfusion, that is a principal denominator of impaired gas exchange, is difficult to monitor routinely in the ICU

An ideal ICU monitoring device should be safe, simple, rapid and deliver reproducible results.
Electrical impedance tomography (EIT) is a non-invasive, non-radiant, continuous technique available at the bedside generating real-time images of impedance distribution within the thorax. Perfusion and ventilation cause variations in thoracic blood and air content, and thus impedance. These variations can be monitored by EIT.
The EIT technique holds substantial promise. To obtain the qualities required for an ideal ICU monitoring device, much further research is needed though.
This thesis - as an initial step - evaluates EIT in experimental physiological and pathological circumstances representative of critical illness.

Electrical impedance tomography

A medical imaging tool based on EIT was first invented by Webster in 1978[1], similar to a technique used in geophysics (electrical resistivity tomography) dating from the 1930s. In addition to geophysics, where electrodes are placed on the surface of earth to locate resistivity anomalies, the technique is used in industrial processes for imaging and monitoring mixture of fluids[2].
The first practical application of a medical EIT system was reported by Barber and Brown in 1984[3,4]. Proposed areas of use include detection of cancer in skin and breast, location of epileptic foci and monitoring of lung function[5,6].

Thoracic applications and monitoring of lung function has been an important field of research for the last decades. The imaging technique has developed quickly recently as a result of progress in computer science. Several clinical and

experimental studies have investigated the use of EIT to study pulmonary ventilation[7-14], whereas fewer have focused on EIT and pulmonary perfusion[15-19]. The more frequent study of ventilation compared to perfusion might be the result of the larger and more easily detected impedance changes induced by ventilation than by perfusion. This is partly because of the different conductivity properties of air and blood and partly because of the much larger tidal volumes compared to stroke volumes measured.
The use of EIT to study ventilation and perfusion in parallel is only scarcely reported[20-22], and the monitoring of ventilation/perfusion matching in endotoxinaemia, does not appear to have been reported previously.
The focus in this thesis is consequently pulmonary perfusion and V/Q matching in both normal physiological and pathological/pathophysiological conditions.

Pulmonary physiology

Pulmonary ventilation

The distribution of pulmonary ventilation is influenced by posture, gravity and mode of ventilation. In the conscious state, ventilation is primarily distributed to the dependent regions of the lung. Gravitational forces are less important in the supine than in the upright position as a consequence of reduced height, resulting in less heterogeneity of ventilation in the supine position. During anaesthesia the uppermost part of the lungs tend to be better ventilated, unrelated to the mode of ventilation[23].
In controlled ventilation, inflation pressure, inflation time, the product of compliance and airway resistance, the time constant tau (τ) determine the degree and rate of alveolar filling. All these factors are commonly altered in pathological conditions requiring ventilatory support.
Compliance, being the volume change per unit pressure change, is low below functional residual capacity (FRC), highest at FRC and decreases again with increasing lung volumes. The total respiratory pressure/volume (P/V) curve, being the sum of chest wall compliance and lung compliance, demonstrates a decrease in total compliance with increasing lung volumes even though chest wall compliance is increasing at higher tidal volumes[24].

Compliance is affected by various pathological conditions including infectious/ inflammatory, fibrotic and oedematous processes.
The airways, including the endotracheal tube, influence airway resistance. The resistance arising from the endotracheal tube can be avoided by direct measurement of tracheal pressure by inserting a pressure line through the endotracheal lumen to the tip of the tube, obtaining tracheal pressure. From this it is possible to derive the pressure affecting the alveoli[25-27].

Regional ventilation has been studied during both physiological and pathological circumstances and may be quantified by inhalation of aerosolised fluorescent microspheres[28], radionuclide scanning by positron emission tomography (PET)[29] and magnetic resonance imaging (MRI)[30,31].
Regional compliance may be computed based on regional tidal volumes using the slice method[32,33], the dynostatic algorithm[34] or in its simplest form by the transpulmonary pressure difference.
An alternative method to describe regional pulmonary filling characteristics has recently been described by Hinz et al[35], calculating the regional filling time versus the global filling time using EIT.

In summary, ventilation is unevenly distributed in the lungs, with gravity being of minor importance compared to its effect on perfusion (described below). Pulmonary structure though, has been reported to be of greater importance for the distribution of ventilation compared to the distribution of perfusion[28] while other data support the theory that the strongest determinant for regional ventilation is regional blood flow[36].

Pulmonary perfusion

Pulmonary circulation differs from systemic in several aspects. Pressures are about one-sixth of systemic pressures (MPAP 15 mm Hg, MAP 90 mm Hg) and the pressure drop in the pulmonary circulation is only one-tenth (MPAP 15 mm Hg to left atrial pressure 5 mm Hg) of the pressure drop in the systemic circulation (MAP 100 mm Hg to right atrial pressure 2 mm Hg). Since blood-flow through the two circulations is the same, the pulmonary vascular resistance is low, only one-tenth of systemic resistance (100-1000 dyne·sec·cm^{-5}, PVR-SVR).
In the healthy lung blood is not directed to specific areas, the uneven distribution of blood to dependent regions being caused partially by gravity[23,37]. Dependent areas hold in addition more and smaller alveoli, compared to the larger and fewer alveoli seen in other parts of the lungs. This could to some extent explain the predominance of perfusion to the dependent parts of the lung[23].
In the diseased lung blood flow is regulated by hypoxic pulmonary vasoconstriction. Blood is directed away from the poorly ventilated lung areas by smooth muscle contraction in the walls of the arterioles[23].

The description of pulmonary perfusion as homogenous gravitational zones by West[38,39] is challenged by more recent investigations, stating both regional and spatial heterogeneity in regional blood flow[40-44].
The uneven distribution of perfusion is believed to be related to a spontaneous temporal variability and a fractal distribution of blood[42,45]. Temporal clusters are asserted to be spatially related and a steal phenomenon, where a simultaneous

increase in flow to one cluster is matched by a decrease in flow to other clusters, is seen at the regional level[43].
These observations could be explained by a hierarchical regulation of regional pulmonary perfusion within the pulmonary vascular tree[43].
As a consequence there is a more heterogeneous distribution of perfusion compared to the distribution of ventilation, within the lungs.

V/Q matching

Ventilation-perfusion ratios determine gas exchange in all single lung units. In the healthy lung ventilation and perfusion are closely matched for optimal gas exchange. This match might result from anatomic relations between airway and vascular structure and/or tightly organized regulation of vascular and bronchiolar tone[36]. In pathological circumstances when regional ventilation or perfusion changes, or both in different magnitude or opposite directions, V/Q ratios turn more heterogeneous and impairment of gas exchange follows.
Intrapulmonary shunting and alveolar dead space are the two extremes of V/Q impairment, shunting representing a V/Q of 0 and dead space representing a V/Q of infinity. The Riley three-compartment model[46], describes the lung divided in three functional compartments where one compartment is both ventilated and perfused (the "effective" compartment). The second compartment is ventilated but not perfused, representing alveolar dead space, and the third compartment is perfused but not ventilated, representing alveolar shunt. This schematic model remains a valid tool for understanding gas exchange in healthy as well as diseased lungs.
Global pulmonary blood flow may be calculated by the Fick CO_2-rebreathing method, thermodilution technique[47,48] or by multiple inert gas elimination technique (MIGET)[49,50]. Regional pulmonary blood flow and V/Q matching may be assessed by radionuclide scanning[29] or MRI[30,31]. Electrical impedance tomography compares favourably with these techniques because of its relative ease of operation, low cost and lack of invasiveness and radiation.

Acute lung injury and sepsis

Acute lung injury

Acute lung injury (ALI) is a clinical syndrome, its most severe form being the acute respiratory distress syndrome (ARDS). ALI is defined by acute hypoxaemic respiratory failure, bilateral oedematous pulmonary infiltrates and normal cardiac filling pressures[51-53]. The mechanisms initiating and propagating lung injury are still not fully known despite extensive investigation.
The incidence of ALI has been reported to be 17.9 per 100,000 in Scandinavia[54], up to 78.9 per 100,000 in the United States with mortality rates between 32 and 50% in several studies[53,55-57]. The large differences in incidence may be explained by

variations in study design, differences in availability of intensive care services in the regions studied, the complexity of the syndrome and diagnostic criteria used.
ALI induced by endotoxinaemia is characterised by pulmonary vasoconstriction[58], impairment of hypoxic vasoconstriction[59] and atypical distribution of perfusion[60]. Regional ventilation changes, secondary to increased airway resistance and decreased pulmonary compliance[61], combined with distorted perfusion result in increased V/Q heterogeneity and impaired gas exchange[62-64].
Endotoxinaemia is in addition frequently observed during ARDS[65] and may contribute to V/Q heterogeneity associated with ARDS[66,67].
Clinical signs of V/Q mismatch and impaired gas exchange are in particular hypoxaemia (PaO_2 < 8.0 kPa or 60 mmHg or oxygen saturation < 90 %) and hypercapnia ($PaCO_2$ > 6.1 kPa or 46 mmHg)[23].

Sepsis

Sepsis is a clinical syndrome, its most severe form being septic shock characterised by acute circulatory failure with arterial hypotension despite volume resuscitation. Sepsis is defined by the presence of both an infectious process and a systemic inflammatory response, severe sepsis furthermore includes organ dysfunction[68].
Severe sepsis and septic shock are frequent indications for admission to ICU and a major cause of morbidity and mortality in critically ill patients[68-70].
Mortality rates vary between 10-50%[70,71], with an ICU mortality in the lower range (15.5%) recently reported in the Finnsepsis study[72].
The sepsis syndrome is complex and highly heterogeneous in terms of cause and expression, in addition to clinical treatment and management differing with geographic regions.
Incidence rates for severe sepsis are equally divergent, from 0.38/1000 inhabitants in the Finnsepsis study[72] to 0.77/1000 inhabitants in Australia and New Zealand[73] and 3.0/1000 inhabitants and 2.26/100 hospital discharges in the United States[70].

The renin-angiotensin system and ALI and sepsis

The classical physiological view of the renin-angiotensin system (RAS) is that of an endocrine system regulating blood pressure and fluid balance. A growing body of evidence suggests that activation of the RAS to generate its principal mediator angiotensin II (Ang II) has many additional effects including regulation of cell growth and fibrosis, inflammation, and endothelial dysfunction. The two receptors described for Ang II, AT_1 and AT_2, are both present at the surface of capillary endothelial cells. They are believed to have different mechanisms of action (figure 1). The AT_1 receptor causes vascular permeability and vasoconstriction by cytoskeletal rearrangement and, via inflammatory mediators for cell adhesion and cell growth, enhances inflammation. The AT_2 receptor has been demonstrated to induce vasodilation, apoptosis and tissue remodelling.

Angiotensinogen, primarily secreted from the liver, is cleaved to produce angiotensin I that in turn is converted to Ang II in the pulmonary circulation, catalysed by angiotensin-converting enzyme (ACE) found on the surface of capillary endothelial cells. There is considerable support for the existence of local systems with all components of the RAS in a number of tissues, including the lung[74,75]. The activity of local pulmonary RAS may be quite different from the endocrine system in settings of ALI/ARDS and inflammatory airway disease[76-78]. The large variability of plasma ACE levels has been attributed to polymorphism (insertion, I, or deletion, D) of the restriction fragment of the ACE gene, the D allele associated with increased ACE activity[79]. Inhibition of ACE has been demonstrated to diminish endothelial activation[80], decrease production of tumour necrosis factor-α[81] and reduce collagen deposition[82]. The results on the association between ACE I/D polymorphism and outcome in severe sepsis and ARDS have been ambiguous, with some studies confirming[83-88] and others rejecting an association or being inconclusive[89,90].

Experimental evidence suggests that activation of pulmonary RAS may influence the development and progression of ALI and ARDS through several pathways including fibrogenesis[82], apoptosis of endothelial[91] and alveolar epithelial cells[92], increased production of tumour necrosis factor-α and interleukins[93,94].
Several studies investigating the role of ACE-inhibitors by blocking the inflammatory pathways involved in the development of ALI/ARDS has been performed. The ACE-inhibitors captopril[95] and enalapril[81] exhibited beneficial effects on pulmonary hypertension in studies involving rodents, while captopril did not alter pulmonary vascular response to hypoxia[96]. The selective AT_1 antagonist losartan, was found to attenuate endotoxinaemic acute lung injury in an experimental study[97] and the same antagonist improved lung injury in an endotoxin-induced shock model[98].

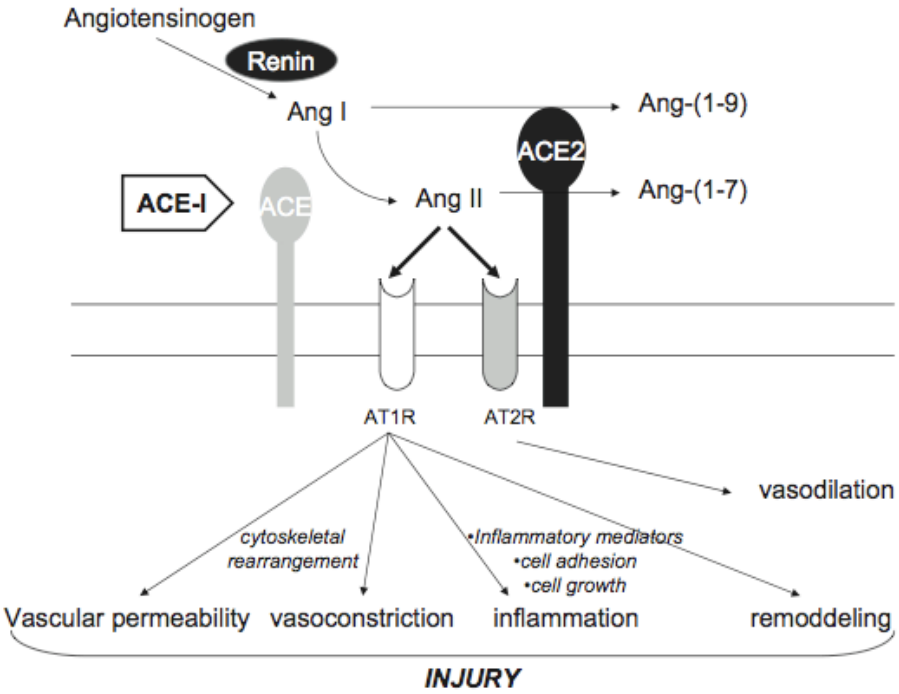

Figure 1. The two receptors described for Ang II, AT_1 and AT_2, and their mechanisms of action.

AIMS

The overall aim of this thesis was to evaluate EIT to monitor pulmonary perfusion and distribution and matching of ventilation and perfusion during both physiological and pathological conditions.

The specific aims were:

- to evaluate global EIT measurements in determining pulmonary perfusion in relation to SV (paper I)
- to assess regional pulmonary perfusion distribution and V/Q matching by combined EIT measurements (paper II)
- to compare global EIT V/Q measurements to standard measurements for venous admixture and dead space (paper II)
- to investigate the applicability of regional EIT to determine distribution and V/Q matching in an endotoxin-induced acute lung injury (ALI) model (paper III)
- to assess the V/Q heterogeneity in an endotoxin-induced ALI model (paper III)
- to apply EIT to investigate the effects of angiotensin-converting enzyme (ACE) inhibition in an endotoxin-induced ALI model (paper IV)

MATERIALS AND METHODS

Animals

All studies were approved by the Ethics Committee for Animal Experiments, the University of Gothenburg, Sweden. Animal care conformed to the principles set forth in the ”Guide for the care and use of laboratory animals” (National Academy of Sciences, ed. 1996, ISBN 0-309-05377-3).

Pathogen-free Swedish landrace pigs of either gender were used in all studies. Study I included eight animals (32-34 kg) and study II six animals (32-34 kg). Two animals contributed with a limited dataset in both studies (I and II).
Study III included eleven animals (30-36 kg) whereas study IV included two groups of animals: ten animals treated with ACE-inhibitor (30-35 kg) and six control animals (30-36 kg).
The size and anatomy of the pigs made it possible to use the same monitoring equipment in the laboratory as in the intensive care unit and total blood volume of the pigs allowed for repeated blood sampling.

Anaesthesia

The animals were fasted overnight with free access to water. To minimise stress, premedication with ketamine and midazolam given intramuscularly, was performed in the boxes housing the animals. Once sedated, animals were moved to the laboratory where anaesthesia was induced with an intravenous bolus of sodium pentobarbital and maintained by an infusion combined with fentanyl. Maintenance crystalloid volume was infused at 10 $ml \cdot kg^{-1} \cdot h^{-1}$ throughout the protocol.
A tracheotomy was performed and the animals were mechanically ventilated in a volume-controlled mode with tidal volume set at 10 ml/kg. Respiratory rate was adjusted to maintain normocapnia.
All animals were investigated in the supine position and their body temperature maintained using heating blankets.

Preparation

A pulmonary artery catheter (PAC) was inserted via the right internal jugular vein to monitor cardiac output (CO), pulmonary arterial pressure and to sample mixed venous blood gases. An arterial line was inserted into the left femoral artery to

monitor arterial pressure and heart rate and for sampling of blood gases. Central venous access to administer fluids and endotoxin was secured via the left jugular internal vein.
A Fogarthy embolectomy catheter was positioned in the inferior caval vein to mimic acute hypovolemia when inflated (study I and II).

To measure tracheal pressure, an air-filled pressure line (outer diameter 1.6 mm) was inserted into the tracheal tube and positioned at the tip of the tube[24,26,27,99] (study I and III).
Oesophageal pressure was measured via a fluid-filled gastric tube (12 Ch) in oesophagus, positioned to minimise cardiac artefacts and to maximise respiratory pressure readings[24,100] (study III).
Measurements of flow and volume were performed using Datex-GE spirometry (based on D-lite^{TM}) and pressures (airway P_{aw}, tracheal P_{tr}, oesophageal P_{oes}) were measured using pressure transducers positioned at the mid-nose level (study III). Lung mechanical measurements were synchronized with the EIT curves using custom designed software (Testpoint^{TM}, Measurement Computing Corporation, Norton, MA) (study III).
Volume dependent compliance (VDC), derived from transpulmonary pressure (P_{tp}), was based on the slice method, using multiple linear regression (MLR) to calculate volume-dependent respiratory system compliance within the tidal volume during ongoing mechanical ventilation[32,33]. The slice method is non-invasive and does not require changes in or special manoeuvres of the ventilatory pattern. The tidal volume studied was divided into ten slices analysed using MLR to create a VDC curve. The tidal volume was divided into three portions and analyzed separately for the low (VDC_{low}), middle (VDC_{mid}) and high (VDC_{high}) volume parts of the tidal breath. The uppermost and lowermost 5% of the pressure-volume loop were excluded[32].
Regional chord compliances ($ROI_{compl\ 1\text{-}4}$) were calculated as P_{tp} − end-expiratory pressure divided by the regional tidal volume derived from EIT measurements (study III).

Functional residual capacity (FRC) was analysed by a modified washin/washout technique[101]. Inspiratory and end-tidal analyses of O_2 and CO_2 concentrations were performed using side stream analysis.
All hemodynamic and respiratory data were monitored using the AS/3 modular monitor system and registered by S/5 Collect software.

Electrical impedance tomography

Electrical impedance tomography is a non-invasive, non-radiant, portable monitoring tool allowing bedside examinations and continuous real-time monitoring of impedance distribution changes within the thorax.

Impedance (Z), measured in ohm (Ω), is the opposition to an alternating current composed of two components perpendicular to each other, resistance (R) and reactance (X). Impedance is a complex number, resistance being the real part and reactance being the imaginary part, describing the resistivity characteristics of electrical circuits and biological tissues. The reciprocal of resistivity is conductivity. The physical impedance principles have recently been reviewed by Bodenstein et al[102].
Impedance can be quantified as:

$$Z = \sqrt{R^2 + X^2}$$

Biological tissues hold different electrical properties and hence impedance and resistivity values (table 1). Blood hold a small resistance and impedance compared to the much higher values obtained for air filled tissues. The very different impedance characteristics of blood and air are important factors when discussing the origin of impedance changes measured.

Impedance measurements can be achieved by three distinct approaches, the most successful and used in clinical practice as well as in our studies being titled dynamic EIT, functional EIT or the relative approach.
The second approach named absolute EIT, anatomical or static EIT is currently not producing good enough images to be in clinical use[7,102-104].
The third, recently developed approach named multifrequency EIT, quasi-static EIT or EIT spectroscopy use multiple frequencies and produce different kinds of EIT images. The interpretation of such images and the benefit of the multifrequency technique yet are to be determined[7,102].

To perform EIT measurements a 16-electrode silicone belt circumscribing the pig mid-thorax is connected to the EIT monitor (EIT Evaluation Kit 2, Dräger Medical, Lübeck, Germany) to generate tomographic images of impedance distribution. A small current of 5 mA and 50 Hz is injected through one of the electrode pairs and the resulting voltage difference measured in all other electrodes (figure 2). The injection of current is repeated sequentially around the thorax creating several images summarised into a final tomographic image (figure 3).

The final image, summarised by dynamic EIT, is compared to a previously recorded reference image, giving the output image regional pixel values of local tissue impedance from baseline i.e. the reference image. The EIT signal is therefore dimensionless and measured in arbitrary units (AU).
In dynamic EIT, only regions exhibiting change of impedance are represented in the images, in contrast to static EIT, where images of absolute conductivity distribution within the thorax are created. Thus, pre-existing areas of consolidated lung secondary to, e.g. pneumonia or atelectasis, will not be recognised as lung tissue employing dynamic EIT[104].

This equation calculates the relative impedance change used in dynamic EIT measurements[102]:

$$\Delta Z_{REL}(t,x,y) = \frac{Z(t,x,y) - Z_{BL}(x,y)}{Z_{BL}(x,y)}$$

ΔZ_{REL} is the resulting impedance change, Z is local impedance, Z_{BL} is mean local impedance during baseline, t is number of tomogram at a certain time point, x and y are positions in the two-dimensional matrix of the EIT image.

Algorithms used to reconstruct the images of dynamic EIT are less sensitive to noise, unequal spacing of electrodes and the non-circular form of the chest, compared to static EIT[7]. A newly developed algorithm for the EIT device used in this thesis is based on a modified "finite element model" where the tissue is divided into triangular-shaped elements (figure 4). The impedance distribution of the elements is modified repeatedly until the best matching with the measured values is seen[8].
Every image consists of more than 200 pixels recorded with a frequency of 10 Hz (depending on the equipment used a frequency range of 10-40 Hz is feasible). The thickness of the studied thomographic slice is about half the thoracal diameter, approximately 10 cm[103,105].
The pig and human mid-thoraces differ in anatomy; lungs respectively exhibit distinct size and characteristics in cross-sectional planes generating distinctly different EIT images (figure 5).
Functional EIT images describe the process of compressing the time course of information into a colour-coded image showing the standard deviation or breath-by-breath tidal differences of impedance change for each pixel on a colour scale (figure 5)[8].

Spatial resolution of EIT varies from one device to another, depending on number of electrodes, signal-to-noise ratios settings employed. In a 16-electrode system, the average resolution in the periphery of the lung is 12 % of the thoracic diameter and in the central regions 20 %. For an adult person, this resolution corresponds to approximately 1.5-3 cm in the cross-sectional plane and 7-10 cm in the craniocaudal direction[104].
Present improvements in EIT devices involve increased spatial resolution, although still not competing with computer tomography or magnetic resonance imaging in performance. On the contrary, the advantage of EIT is primarily the improvement in temporal resolution making it possible to monitor impedance changes over time in detail.

Table 1. Resistivity values (Ω cm) for intra-thoracic tissues. Note the large difference between air and blood.

Resistivity values	Tissue
1 x 10^7	***Air***
400	Heart muscle
2000	Heart fat
1400	Lung
2000	Bone
2000	Cartilage
150	***Blood***

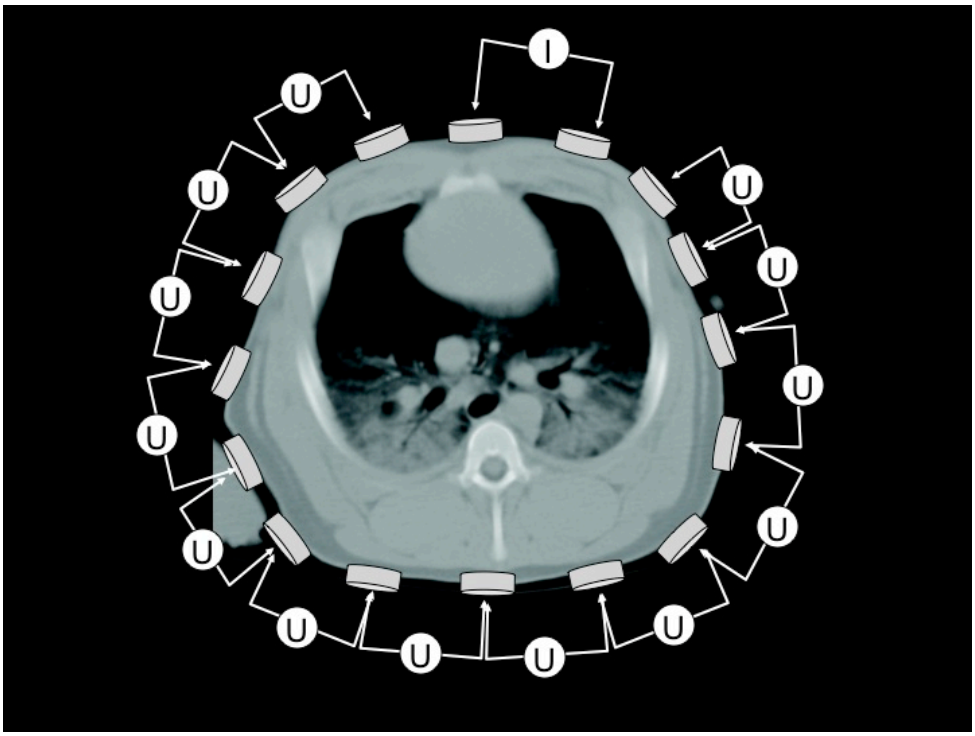

Figure 2. Drawing of 16 EIT electrodes circumscribing the pig mid-thorax. Example of current injected (I) in two adjacent electrodes and resulting voltage differences (U) measured in all other electrodes

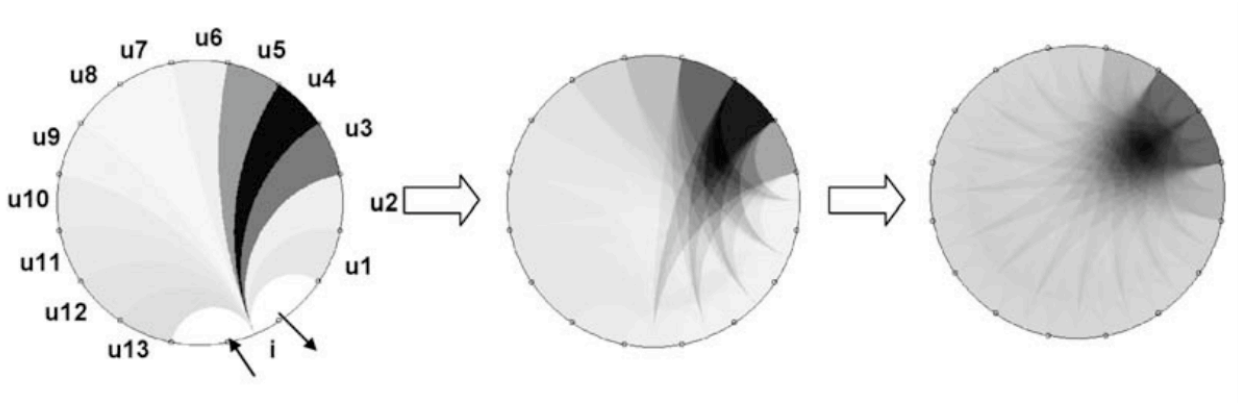

Figure 3. Injection of current (i) (left) through adjacent electrode pairs repeated sequentially around thorax to create several images (middle) summarised into a final tomographic image (right). (Putensen et al, Electrical impedance tomography guided ventilation therapy, Curr Opin Opin Crit Care 2007; 13: 344-50, Printed with permission from Lippincott Williams & Wilkins, Inc.)

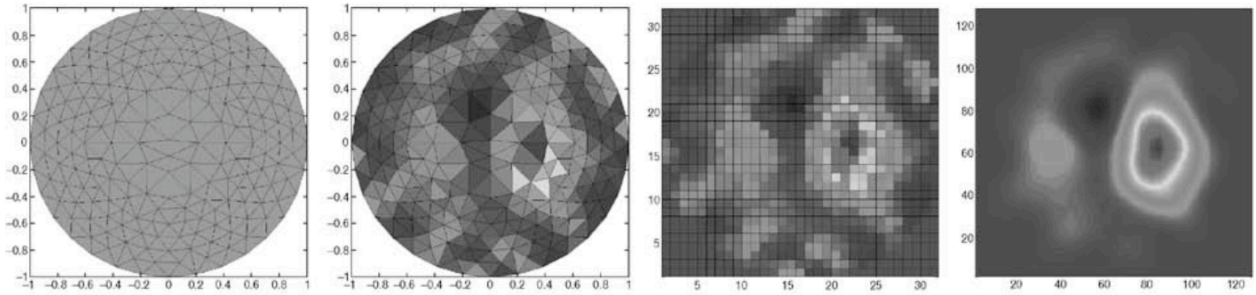

Figure 4. "Finite element model" where the pig thorax is divided into homogeneous triangular shaped elements. The impedance distribution of the elements is repeatedly modified to minimise the difference between the theoretical model and the actual measurements. (Putensen et al, Electrical impedance tomography guided ventilation therapy, Curr Opin Opin Crit Care 2007; 13: 344-50, Printed with permission from Lippincott Williams & Wilkins, Inc.)

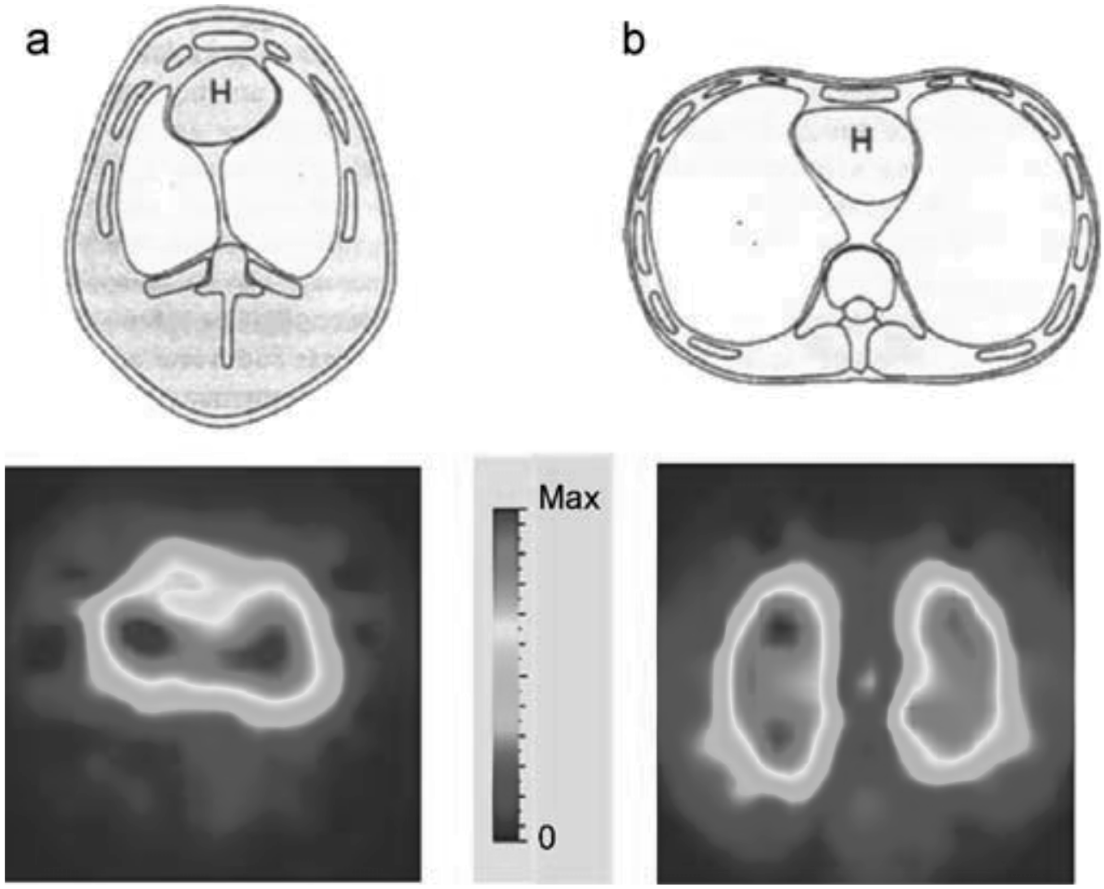

Figure 5. Cross sectional diagrams of pig (a) and human (b) mid-thorax and the corresponding functional EIT images. (Meier et al, Electrical impedance tomography: changes in distribution of pulmonary ventilation during laparoscopic surgery in a porcine model, Langenbecks Arch Surg (2006) 391: 383-389, Printed with permission from Langenbecks Arch Surg.)

In this thesis the unfiltered EIT signal was recorded, the files converted to ASCII format using dedicated EIT software (Drager EIT Data Review version 4 in studies I and II, version 5 in studies III and IV) and then analysed offline using custom-made software. The amplitude, as the mean ± one standard deviation, of impedance changes (ΔZ) was calculated during ongoing ventilation (Z_V, the mean of 5-8 breaths) and during a short apnoea (Z_Q, the mean of 15-25 pulse beats during an expiratory pause). Pulse synchronous impedance changes can be seen superimposed on the much larger ventilation-induced impedance changes but are more easily discernable during apnoea. All perfusion measurements are therefore recorded during a short apnoea (figure 6).

Regional differences in impedance change within the lungs are possible to study using the EIT software for regions of interest (ROI). Regional measurements of the anterioposterior axis in the lung fields for the left and right lungs respectively are

described in study II, III and IV (figure 7). Before start of study protocols the tidal volume was increased and decreased by 100 ml to allow for a volume calibration of the associated changes impedance (study I).

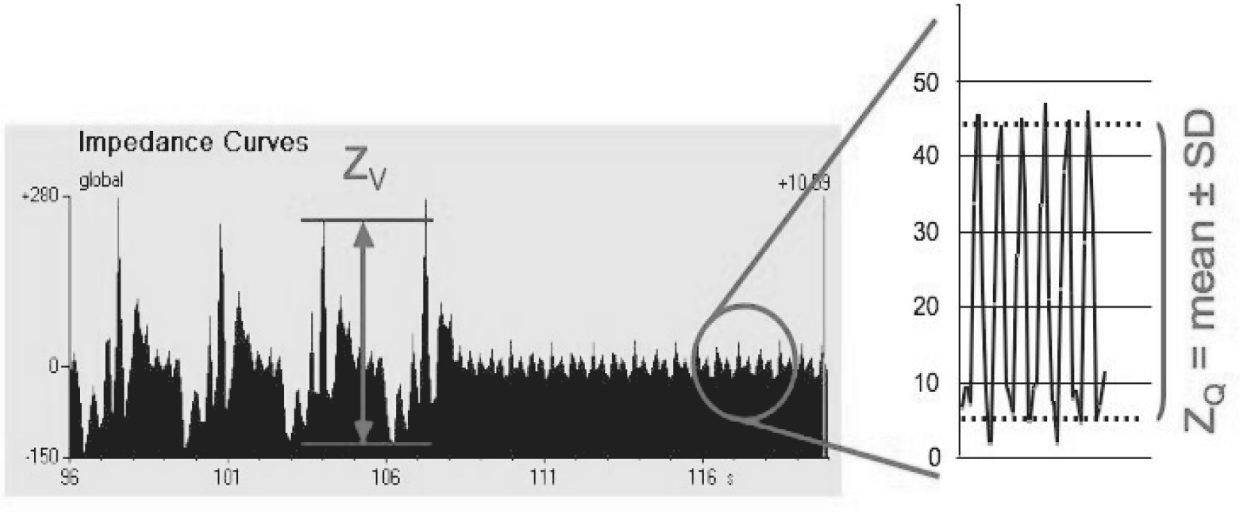

Figure 6. Graphical presentation of an EIT recording with large impedance amplitudes, Z_V, during ongoing ventilation and small amplitudes related to perfusion, Z_Q, easily detected during apnoea. The systolic impedance amplitude, ΔZ_{sys}, is measured as the mean ± SD.

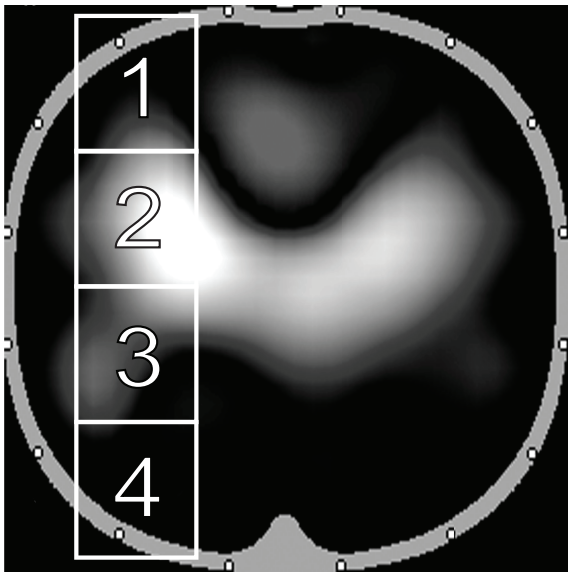

Figure 7. EIT image of a pig mid-thorax displaying regions of interest (ROIs) of the right lung. ROI 1 = anterior, ROI 2 = mid anterior, ROI 3 = mid posterior and ROI 4 =posterior parts of the lung. Note the position of the heart.

Experimental design

All animals were allowed to rest for one hour following preparation. A complete set of hemodynamic, respiratory and EIT data recordings completed with blood gas analyses were made at baseline (BL).

Interventions in study I

Several cycles of measurements were performed in random order reducing CO either by inflating the balloon of the Fogarthy catheter or increasing PEEP from 5 to 10 or 20 cm H_2O. The balloon was inflated to reduce CO by more or less than 50% of BL to achieve a wide range of results in CO and thus pulmonary perfusion. EIT recordings, haemodynamic measurements and arterial blood gases were completed before and after each intervention during a short apnoea as described above. EIT measurements were made during apnoea to determine pulse-synchronous systolic changes in impedance (ΔZ_{sys}). Synchronisation of the EIT signal and the systemic, pulmonary artery and tracheal pressures was achieved using the initiation of ventilation after apnoea as the fixed time point.

Interventions in study II

Cardiac output was reduced by inflating the balloon of the Fogarthy catheter or by increasing PEEP from 5 to 20 cm H_2O. Blood samples were collected (arterial and mixed venous) and analysed and respiratory data were noted. EIT measurements were made during both ventilation and apnoea to generate images of ventilation- (Z_V) and perfusion-induced changes (Z_Q) in thoracic impedance. Four rectangular, equally sized regions of interest (ROIs) of 8 by 4 pixels each were set along either the left or the right lung axis covering the lung fields, carefully positioned not to include the cardiac area (figure 7). The ROIs extended the full ventral to dorsal distance, representing the ventral (ROI 1), mid-ventral (ROI 2), mid-dorsal (ROI 3) and dorsal (ROI 4) parts of either lung.

Interventions in study III

After BL measurements an infusion of Escherichia coli lipopolysaccharide (Serotype 0111:B4, Sigma chemical Co, USA) was started. The initial dose of 2.5 µg/kg/h was doubled every 10 minutes to 20 µg/kg/h at 30 minutes and then maintained at this infusion rate for two hours. Volume resuscitation using 500-750 ml of hydroxyethyl starch (Voluven, Kabi-Fresenius, Solna, Sweden) targeting restoration of baseline CO was given once full dose of endotoxin infusion had been established. EIT measurements were performed as in study II.
Collection of a complete set of data was made every 30 minutes throughout the protocol (T30, T60, T90, T120, T150).
Measurements of flow, volume and pressures (airway P_{aw}, tracheal P_{tr}, oesophageal P_{oes}) were collected every 30 minutes during the endotoxin infusion protocol.

Interventions in study IV

Animals were randomised to receive a bolus of 5 mg enalapril (Sigma-Aldrich Sweden AB, Stockholm, Sweden) (ENAL, n=10) or the saline vehicle (CTRL, n=6) after completing the preparation. Baseline measurements and EIT recordings were performed 30 minutes after the administration of enalapril/saline followed by start of endotoxin infusion according to the protocol described for study III. Volume resuscitation was performed as in study III. EIT measurements were performed as in study II. Collection of a complete set of data was made every 30 minutes for two and a half hours as in study III (T30, T60, T90, T120, T150).

Western Blot technique (study IV)

Animals were killed at the end of the protocol following deepened pentobarbital anaesthesia using a saturated potassium-chloride solution. After immediate sternotomy, bilateral lung biopsies were collected and snap-frozen in liquid nitrogen. The tissue samples were prepared and analysed by Western Blot technique for the expression of Ang II receptors 1 and 2 (AT_1 and AT_2). The frozen biopsies were sonicated in PE buffer to fragment cells, macromolecules and membranes. The homogenate was centrifuged and the supernatant analysed for protein content by the Bradford method[106] and then diluted in buffer and heated to 70°C before electrophoresis was performed. The proteins were then transferred to a membrane incubated with AT_1 and AT_2 receptor antibodies and a substrate containing specific anti AT_1 and anti AT_2 IgG antibodies was used to identify the immunoreactive protein by chemiluminescence. Images were captured by a Chemidox XRS cooled CDD camera and analysed with Quantity One software, then quantified as optical density (OD) per microgram of protein.

Calculations and statistical analyses

All values were reported as the mean and standard deviation (SD) or 95% confidence interval as indicated. Ang II type I receptor quantification was reported as median and 95% confidence interval. Statistical significance was set at $p<0.05$. All statistical analyses were performed using Prism 5 for Mac OSX (GraphPad Software Inc., San Diego, Ca).

EIT measurements

The ΔZ_{sys} was translated to millilitres using the tidal volume calibration data based on the change in impedance for a ± 100 ml change in TV (study I).
Z_V and Z_Q were multiplied by the respiratory rate and the heart rate respectively, to provide a common format in AUs per minute. The relative distribution of Z_V and Z_Q to each ROI was calculated as the proportion of the global, cumulative sum of

ROI 1-4, and the V/Q ratio was calculated from the proportional Z_V/Z_Q ratio (study II, III, IV).
In study II and III the calculated proportions were performed for the left and right lung, respectively.
In study III the cumulative sum of Z_V in ROI 1-4 was divided by the tidal volume to obtain a scaling factor used to translate Z_V in individual ROIs into equivalent fractions of the tidal volume.

Calculations

Venous admixture (Q_s/Q_t) was calculated according to the standard formula based on pulmonary capillary, arterial and mixed venous oxygen contents. Fractional alveolar dead space (V_D/V_T) was estimated by dividing the arterial to end-tidal CO_2 gradient by the arterial CO_2 tension[107] (study II, III, IV).
Transpulmonary pressure, P_{tp}, was calculated as the difference between P_{tr} and P_{oes} and used to calculate volume dependent compliance (VDC) based on the SLICE method.[32,33] The volume dependent compliance was divided in low (VDC_{low}), middle (VDC_{mid}) and high (VDC_{high}) parts of the tidal volume. Regional chord compliances were calculated as the P_{tp} – end-expiratory pressure difference divided by the regional tidal volume (study III).

Statistical analyses

The association between ΔZ_{sys} and stroke volumes (SV) was evaluated using the Spearman rank correlation coefficient because of the non-normality of the data. The relative changes in ΔZ_{sys} and SV from BL were evaluated by Bland-Altman analysis to evaluate the limits of agreement (study I).

Changes in Z_V, Z_Q, their distribution and the Z_V/Z_Q ratios were analysed by paired t-test. Correlations between Z_V/Z_Q ratios by EIT and Q_s/Q_t and V_D/V_T were evaluated using Pearson linear correlation (study II).

Changes over time were analysed by repeated measures ANOVA followed by the Tukey´s multiple comparison test. Correlations of changes were evaluated using within subject analysis[108]. Correlations at one point in time were evaluated by linear regression (study III).

Haemodynamic, gas exchange and EIT variables were analysed by two-way ANOVA using time (BL to T150) and group (CTRL or ENAL) as factors. Western Blot results for Ang II type I were analysed by the Mann-Whitney test (study IV).

REVIEW OF RESULTS

All haemodynamic and gas exchange variables were within physiological limits[109,110] at BL (studies I-IV):

	BL	Bal	BL	PEEP	BL ETX	ETX 150	BL ctrl	ETX 150 ctrl	BL enal	ETX 150 enal
CO (l/min)										
I	2.6 ± 1.0	1.8 ± 0.6	2.7 ± 0.9	2.4 ± 0.8						
II	3.1 ± 0.7	1.3 ± 0.2	3.2 ± 0.9	1.8 ± 0.3						
III					3.2 ± 0.9	4.2 ± 1.0				
IV							3.5 ± 0.7	4.5 ± 1.1	3.0 ± 0.9	4.0 ± 0.9
SV (ml)										
I	21 ± 9	14 ± 5	21 ± 7	18 ± 7						
II	27 ± 5	12 ± 4	27 ± 4	14 ± 4						
III					30 ± 7	31 ± 11				
IV							32 ± 4	35 ± 9	29 ± 8	28 ± 12
MAP (mmHg)										
I	80 ± 32	54 ± 16	93 ± 24	83 ± 24						
II	122 ± 7	50 ± 15	124 ± 11	83 ± 16						
III					105 ± 26	68 ± 9				
IV							110 ± 22	69 ± 5	106 ± 22	33 ± 9
Q_s/Q_t (%)										
I										
II			11 ± 2	5 ± 1						
III					9.1 ± 0.3	34 ± 12				
IV							8.8 ± 2	33 ± 14	9.9 ± 3	36 ± 11
V_d/V_t (%)										
I										
II	9 ± 4	27 ± 11								
III					7.6 ± 7	26 ± 6				
IV							9.1 ± 6	24 ± 4	9.0 ± 4	27 ± 6
A-a diff (kPa)										
I										
II										
III					17 ± 53	238 ± 182				
IV							3.8 ± 1.8	28 ± 24	5.6 ± 1.7	33 ± 26

Study I

A wide range of SV between 5.5 - 36 ml was achieved by the interventions. A significant correlation was found between ΔZ_{sys} and SV for pooled data of the interventions (ρ=0.62) (figure 8) Furthermore, significant correlations were found for the subsets of data on balloon inflation (ρ=0.73) and increased PEEP (ρ=0.40). The Bland-Altman plot of changes relative baseline demonstrated a bias of -7 ± 22% with the 95% limits of agreement being -51% to 36% (figure 9). The calculated SV derived from ΔZ_{sys} correlated to SV derived from the PA catheter with p = 0.50. The best precision was observed for stroke volumes in the range up to 15 ml, deteriorating for larger volumes.

A typical illustration of time-synchronised changes in pulmonary artery pressure and the EIT curve is given in Figure 10. The systolic pressure trace (P_{art}) was associated with reduced impedance with a deflection of the curve coinciding with the dicrotic notch, showing the onset of diastole.

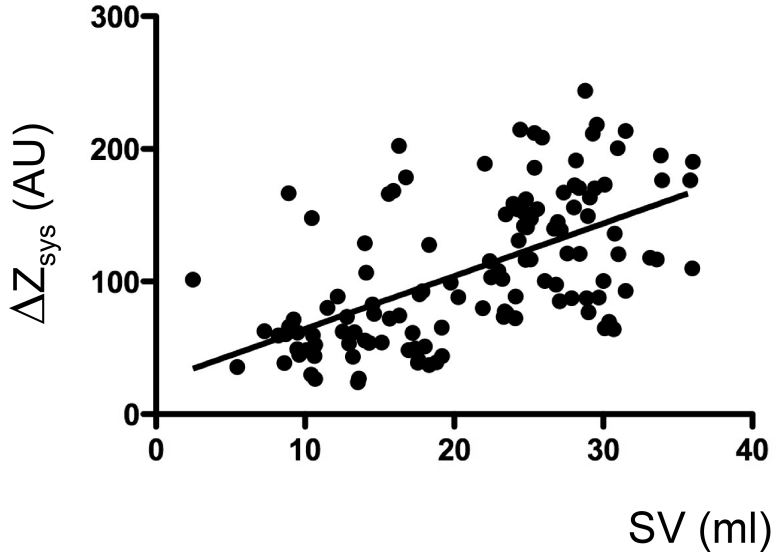

Figure 8. Scatterplot of all SVs determined by the PAC vs. ΔZ_{sys} measured by EIT. Spearman correlation coefficient ρ = 0.62

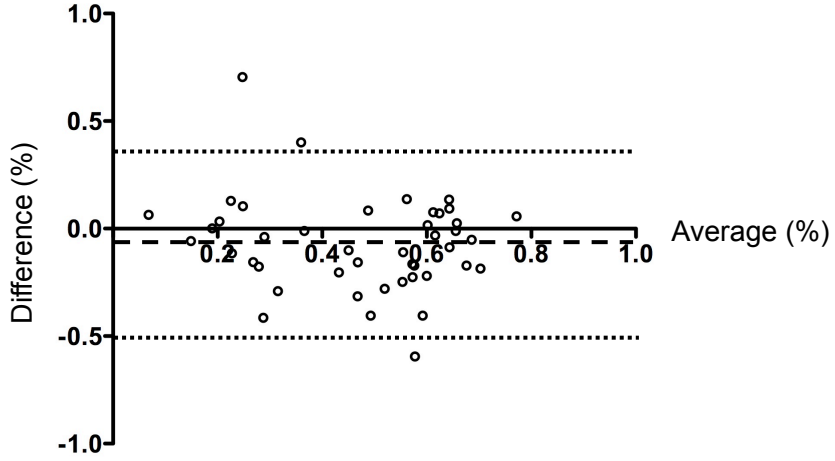

Figure 9. Bland-Altman plot (difference vs. average) of simultaneous relative changes (%) from BL obtained using the PAC and EIT. A bias of -7% (dashed line) with the 95% limits of agreement at -51% and 36% (dotted lines) was demonstrated.

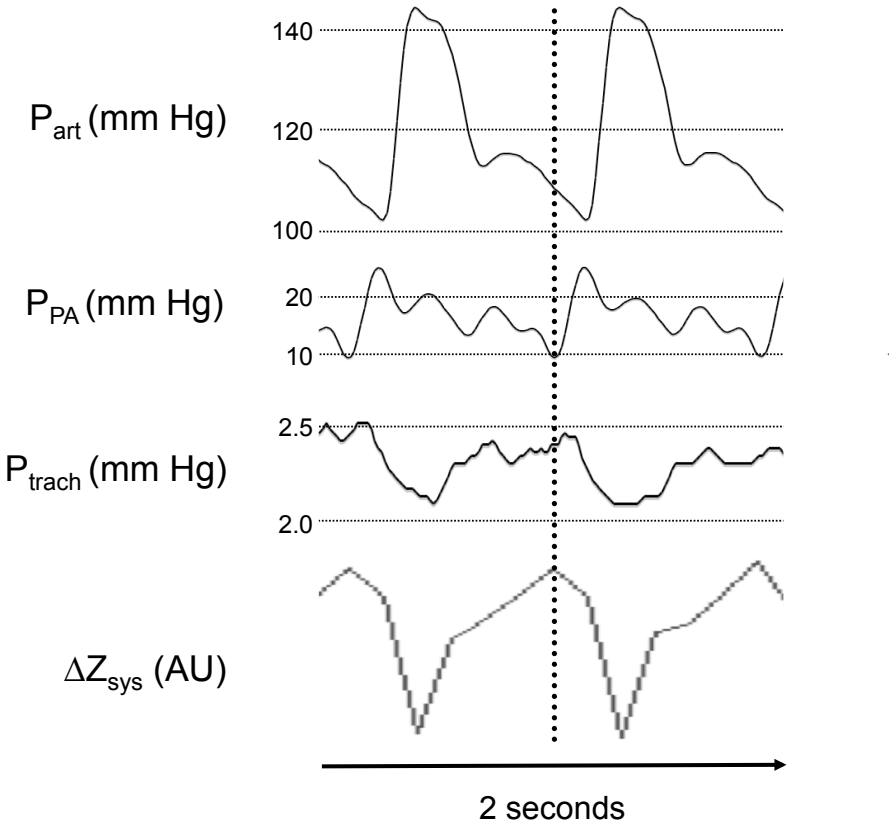

Figure 10. Time-synchronised tracings of arterial (P_{art}), pulmonary arterial (P_{PA}) and tracheal (P_{trach}) pressures, together with the thoracic impedance change (ΔZ_{sys}) during apnoea. The reduction in impedance coincided with the start of pulmonary arterial systole (dotted line).

Study II

At baseline conditions the greatest impedance amplitudes for Z_V and Z_Q were observed in the mid-ventral lung region (ROI 2) for both lungs. Balloon inflation as well as increased PEEP reduced the perfusion induced impedance change (Z_Q) in ROI 2. PEEP increased ventilation induced impedance change (Z_V) in ROI 3 bilaterally.

A parallel distribution of relative Z_V and Z_Q was observed at baseline with the greatest proportion of ventilation and perfusion in ROI 2, followed by ROI 3 and then ROI 1. A minor, although equal part of ventilation and perfusion was seen in ROI 4.
The balloon intervention reduced the proportion of Z_Q in ROI 2 in both lungs and increased the proportional Z_Q in the left ROI 1. No change in the distribution of Z_V was observed.
The PEEP intervention increased Z_V in ROI 3 for both lungs while a decrease was seen in ROI 2. A reduction of Z_Q was observed in ROI 2 (figure 11 and 12).

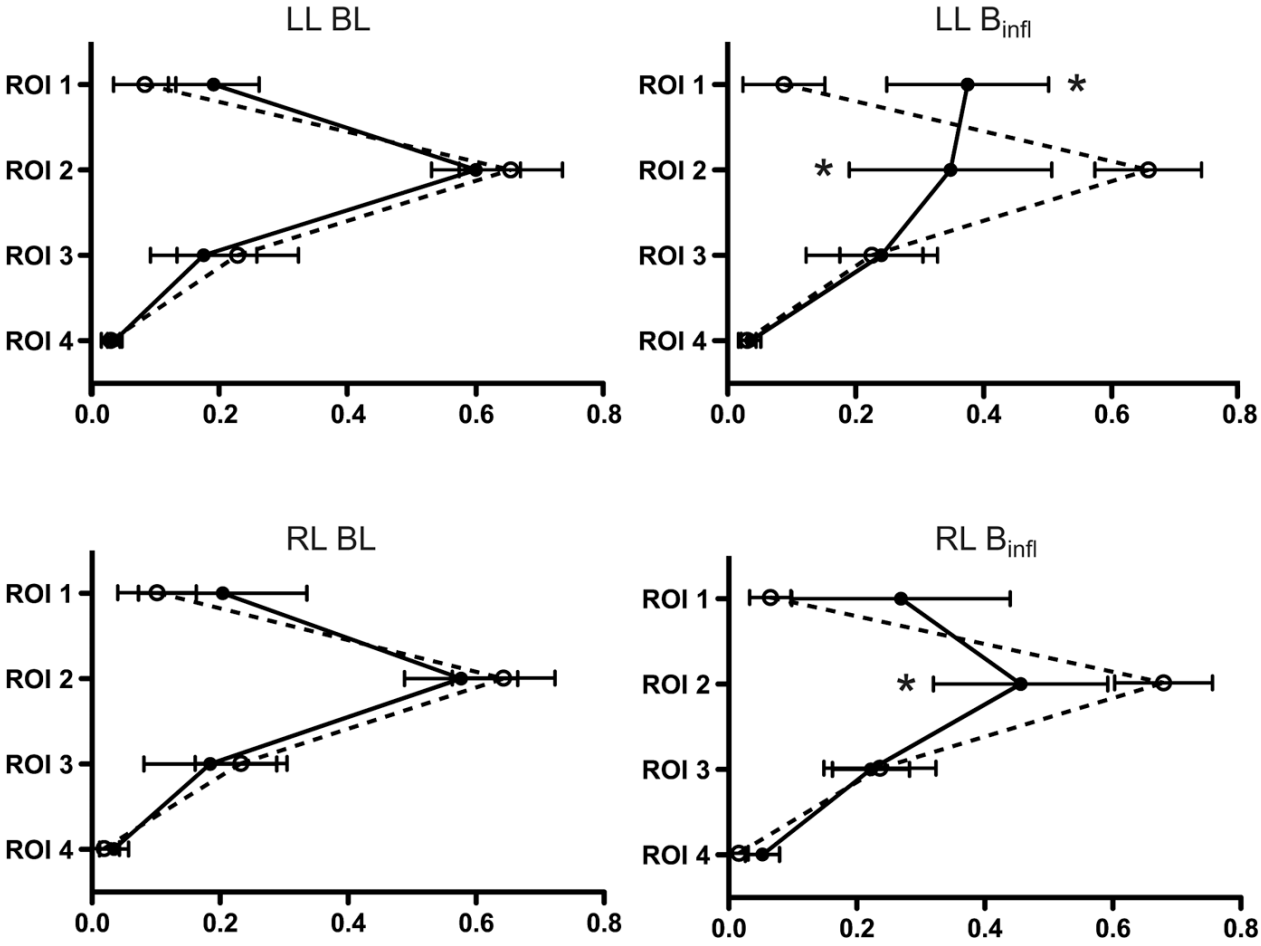

Figure 11. Relative distribution of Z_V and Z_Q (%) within ROI 1 to 4 for the left and right lung, at BL and following balloon inflation. Z_V = dashed line, Z_Q = solid line. * denotes significant difference for Z_Q compared to BL.

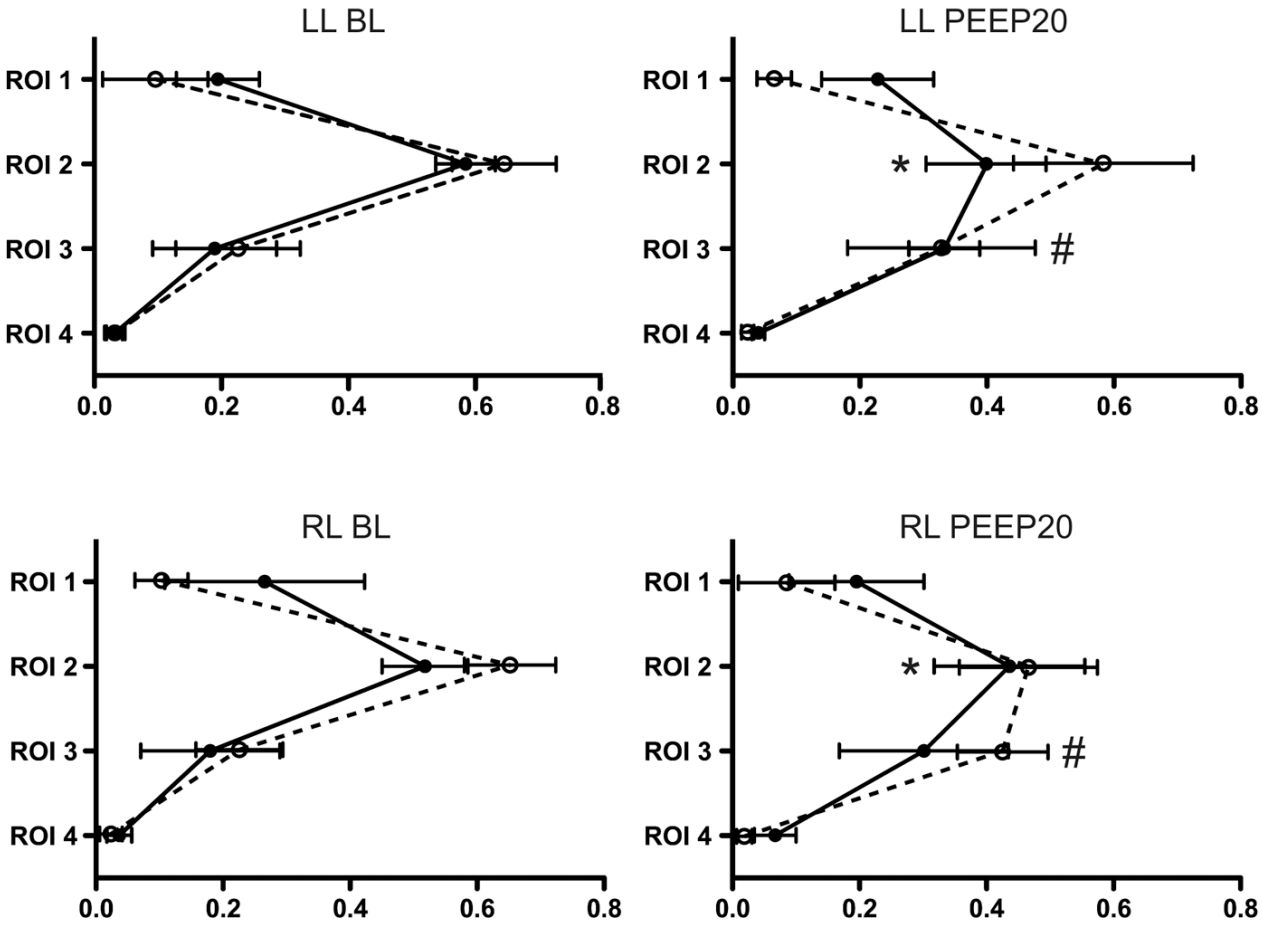

Figure 12. Relative distribution of Z_V and Z_Q (%) within ROI 1 to 4 for the left and right lung, at BL and following the application of PEEP 20. Z_V = dashed line, Z_Q = solid line. * denotes significant difference for Z_Q compared to BL, # denotes significant difference for Z_V compared to BL.

All EIT Z_V/Z_Q ratios at baseline were calculated and their frequency distribution had a Gaussian shape with a mean V/Q of 1.1. This distribution changed into a non-Gaussian pattern after interventions with a mean V/Q of 0.86 (figure 13). Calculated V/Q ratios by EIT correlated to venous admixture ($r^2 = 0.48$) with a negative slope and to dead space fraction ($r^2 = 0.63$) with a positive slope.

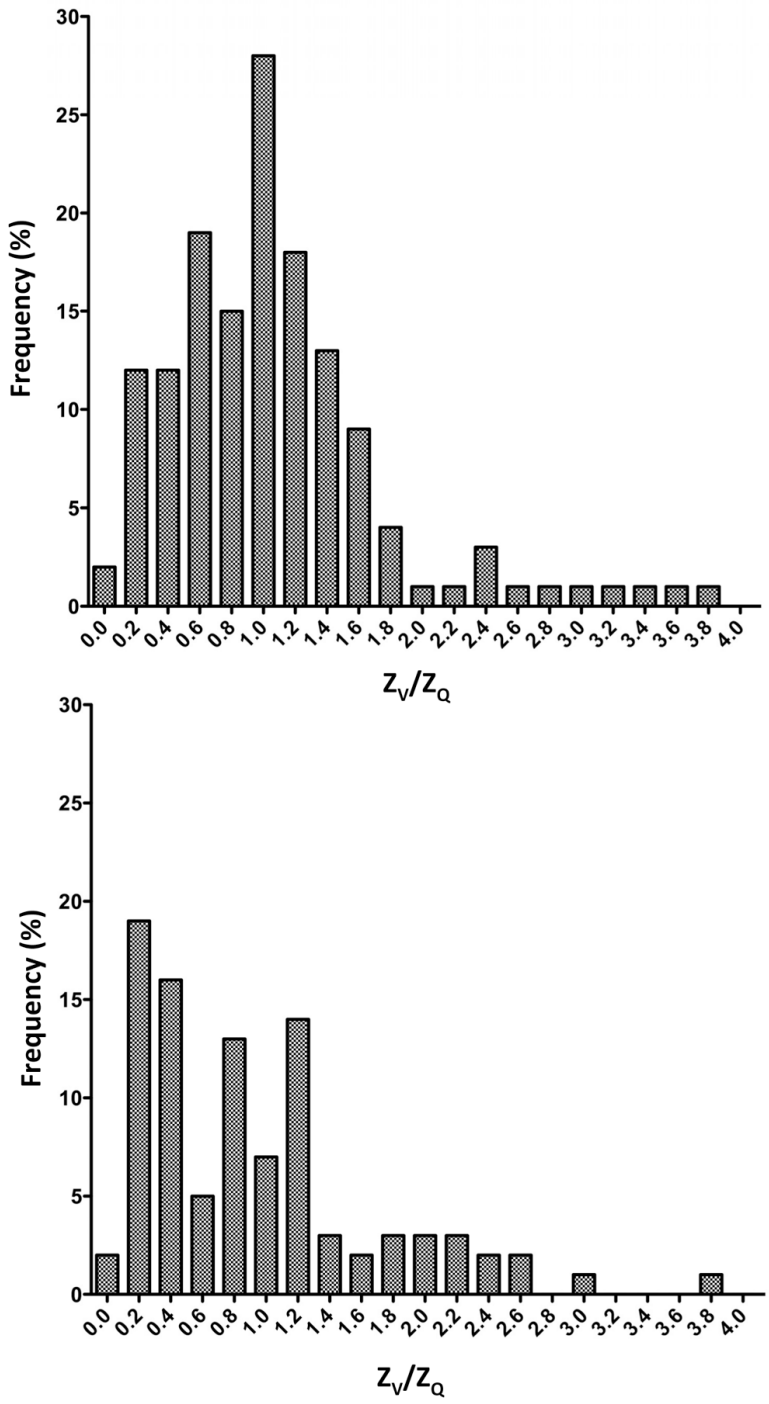

Figure 13. Frequency distribution of Z_V/Z_Q ratios at BL (top) and following interventions: balloon inflation or increase to PEEP 20 (bottom).

Study III

Endotoxinaemia rapidly induced pulmonary hypertension persisting throughout the protocol. Baseline CO was successfully maintained by volume resuscitation and a hypotensive, hyperdynamic circulatory state was reached towards the end of the protocol.
Throughout the entire experiment global perfusion, Z_Q, correlated to SV, as measured by the PAC (r^2= 0.69). When separated for normodynamic baseline measurements and the hyperdynamic final state, the correlations between Z_Q and SV were $r^2 = 0.78$ and $r^2 = 0.71$, respectively.

The linear regression of regional Z_Q in relation to BL as the line of identity successively deteriorated during endotoxinaemia (T30 $r^2 = 0.64$, T60 $r^2 = 0.60$, T90 $r^2 = 0.35$, T120 $r^2 = 0.15$, T150 $r^2 = 0.18$) and consequently the slope progressively decreased. In contrast, neither the linear regression of regional Z_V in relation to BL nor the slope changed significantly during endotoxinaemia (T30 $r^2 = 0.98$, T60 $r^2 = 0.95$, T90 $r^2 = 0.87$, T120 $r^2 = 0.83$, T150 $r^2 = 0.81$) (figure 14).

Endotoxinaemia reduced FRC (603 ml at BL to 471 ml at T150) that correlated with a reduction in global end-expiratory Z_V ($r^2 = 0.74$). Moreover, the reduction in FRC correlated to an increased A-a difference ($r^2 = 0.74$) and increased Q_s/Q_t ($r^2 = 0.55$).
Whole lung compliance successively decreased from VDC_{low} (51 ml/cm H_2O) to VDC_{mid} (43 ml/cm H_2O) and VDC_{high} (32 ml/cm H_2O) at BL. This relation was maintained throughout the protocol with the greatest reduction in compliance appearing in VDC_{high} (55% of BL) at T150, while VDC_{low} and VDC_{mid} were reduced to about two-thirds of BL (figure 15).

Regional chord compliance differed at BL with the greatest compliances in ROI 2 (16 ml/cm H_2O) and ROI 3 (18 ml/cm H_2O) and the least compliances in ROI 1 (8.8 ml/cm H_2O) and ROI 4 (12 ml/cm H_2O). The regional chord compliance progressively decreased during endotoxinaemia, with the largest reduction in the most dependent region while better maintained in the ventral lung (figure 15).

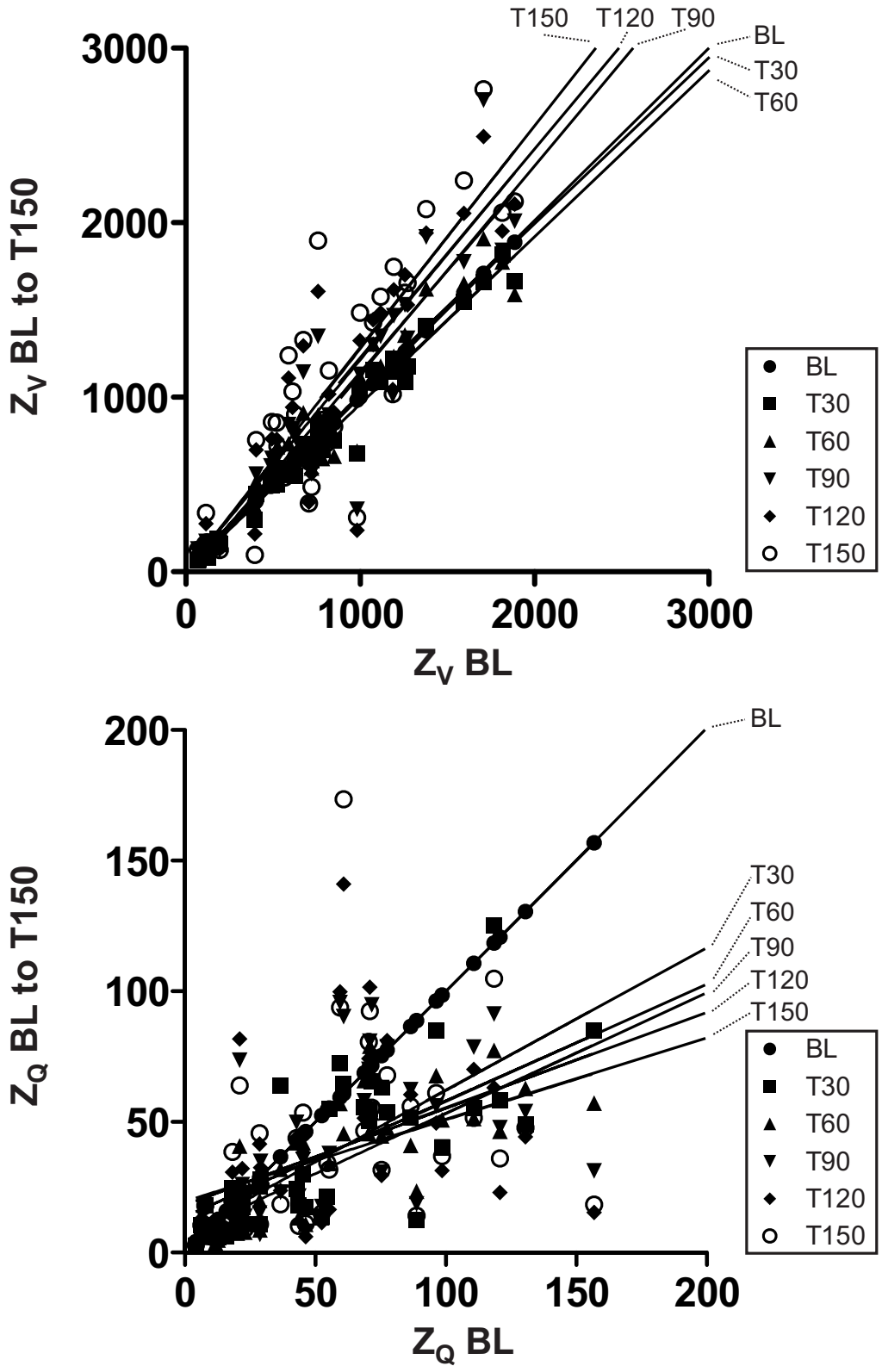

Figure 14. Effect of endotoxinaemia on Z_V (top) and Z_Q (bottom) distribution in relation to BL. All values at each point in time (BL to T150, y-axis) were plotted against the values at BL (x-axis), resulting in the BL as the line of identity. Linear regression lines for each time point are indicated.

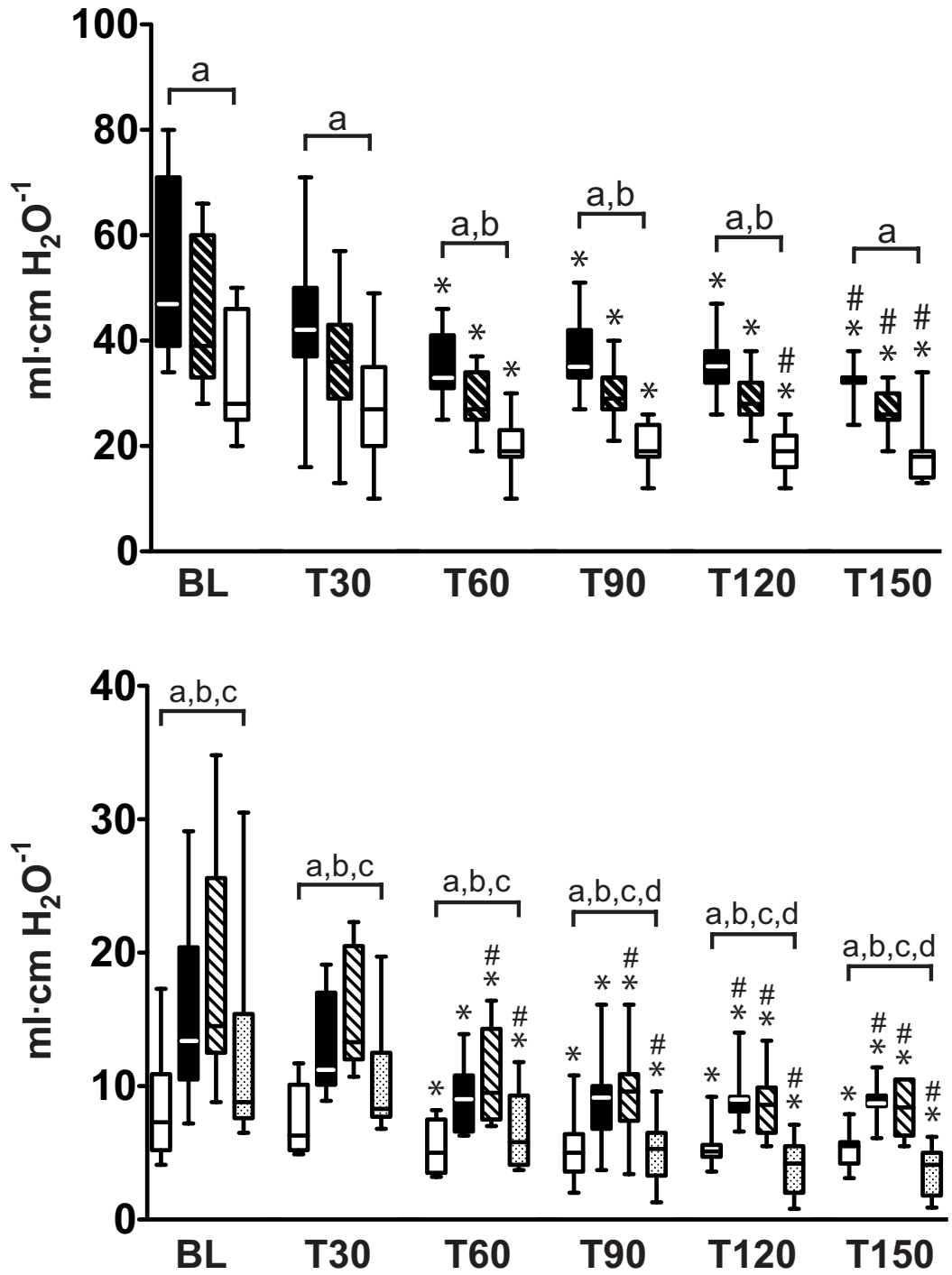

Figure 15. Changes in total VDC (top) and regional chord compliance (bottom) during endotoxinaemia. The top graph shows boxplots of changes in VDC for VDC_{low} (black bars), VDC_{mid} (hatched bars) and VDC_{high} (open bars) from BL to T150. * $p < 0.05$ vs. BL, # $p < 0.05$ vs. T30. a, $p < 0.05$ VDC_{low} vs. VDC_{high}; b, $p < 0.05$ VDC_{mid} vs. VDC_{high}. The bottom graph shows boxplots of changes in regional chord compliance in ROI 1 (open bars), ROI 2 (black bars), ROI 3 (hatched bars) and ROI 4 (grey-dotted bars) from BL to T150. * $p < 0.05$ vs. BL, # $p < 0.05$ vs. T30. a, $p < 0.05$ ROI 1 vs. 3; b, $p < 0.05$ ROI 1 vs. 2; c, $p < 0.05$ ROI 3 vs. 4; d, $p < 0.05$ ROI 2 vs. 4.

The baseline Z_V/Z_Q ratio of 1.1 reflected the largely parallel distribution of ventilation and perfusion with most of both Z_V and Z_Q distributed to ROI 2 and 3. The Z_V/Z_Q ratio in ROI 1 was consistent with dead space ventilation and in ROI 4 the ratio indicated venous admixture (exemplified for the right lung in Figure 16).

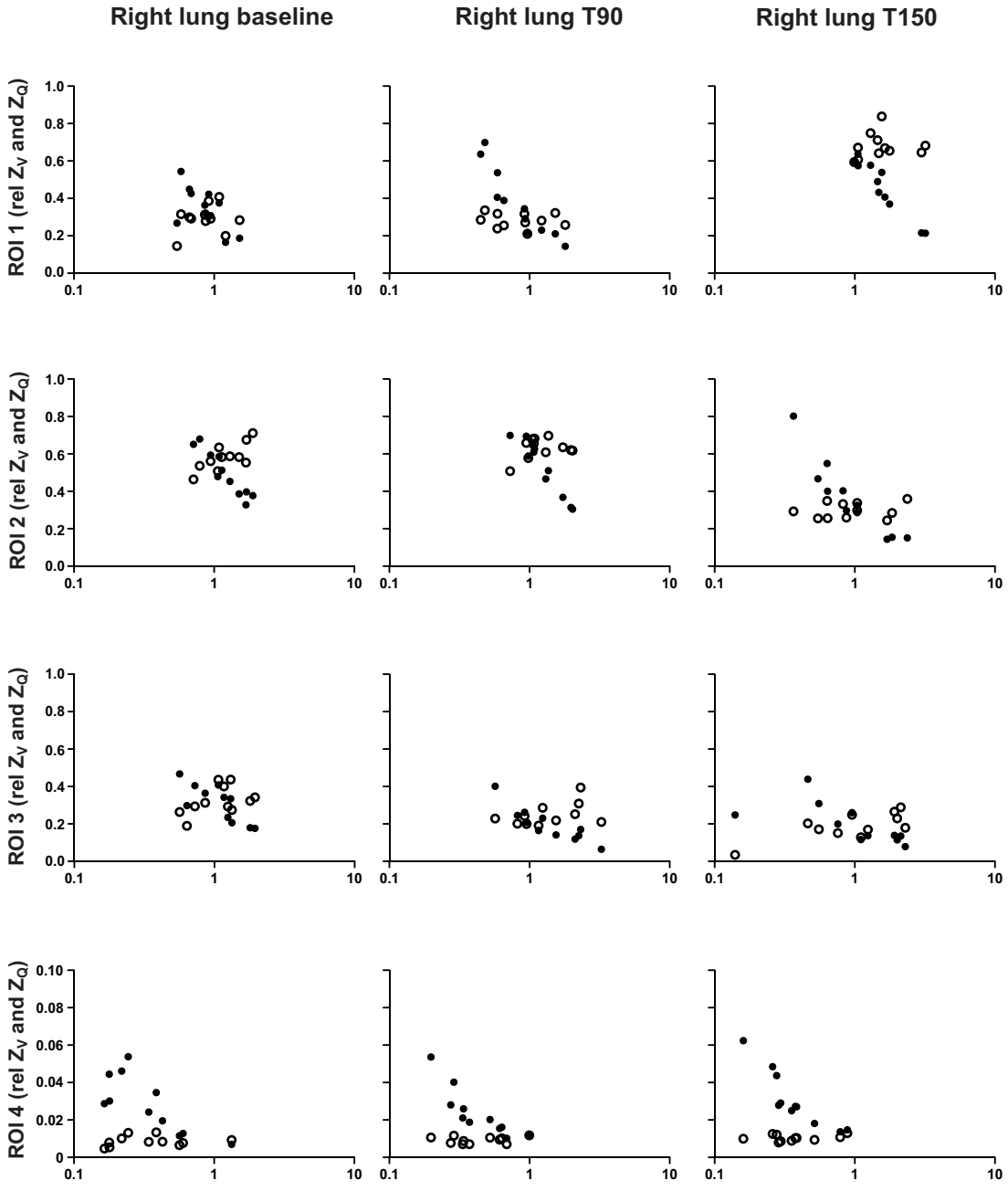

Figure 16. Effect of endotoxinaemia on Z_V/Z_Q matching in the right lung. Scatterplots of Z_V (open circles) and Z_Q (filled circles) and the corresponding Z_V/Z_Q ratio. The relative distributions of Z_V and Z_Q in all ROIs are plotted on the y-axis against the Z_V/Z_Q ratio on the x-axis, at BL, T90 and T150.

Endotoxinaemia induced a ventral shift of ventilation concomitant to a dorsal shift of perfusion. The global V/Q ratio consequently was reduced to 0.83 at the end of the experiment (T 150).
Global Z_V/Z_Q ratios correlated negatively to venous admixture ($r^2 = 0.66$), and positively to dead space fraction ($r^2 = 0.61$) similar to study II, and in addition global Z_V/Z_Q correlated to the alveolar-arterial O_2 difference ($r^2 = 0.65$).

Study IV

Enalapril did not induce any significant haemodynamic changes at baseline. Similar pulmonary artery hypertension and systemic hypotension were observed between ENAL and CTRL animals. No differences were observed between the groups regarding S_vO_2 and CO, that were both well maintained by volume resuscitation following full-dose endotoxin infusion.

Enalapril did not influence the heterogeneity of ventilation nor perfusion induced by endtoxinaemia, although a trend towards heterogeneity was observed in ENAL animals.

The overall Z_V/Z_Q ratio was 1.02 in CTRL animals and 1.05 in ENAL animals with no significant difference between the two groups.
Throughout the protocol Z_V shifted towards the ventral ROI 1 and 2 while Z_Q shifted dorsally. Similar shifts were noted for both CTRL and ENAL animals. At the end of the protocol (T150) the overall Z_V/Z_Q ratio had decreased to 0.77 in CTRL animals and to 0.84 in ENAL animals.
Regional changes consisted of increased venous admixture in the dependent lung areas represented by ROI 3 and 4. Similar results for controls (Z_V/Z_Q from 1.31 and 0.88 at BL to 0.95 and 0.53 at T150) and enalapril treated (Z_V/Z_Q from 1.34 and 0.64 at BL to 0.82 and 0.54 at T150) animals were noted with no significant differences (figure 17, 18).

No differences in the expression of AT_1 receptor in CTRL (21.6 OD/µg protein) and ENAL (19.0 OD/µg protein) animals were detected. The AT_2 receptor was not detectable in relevant amounts in any group of animals.

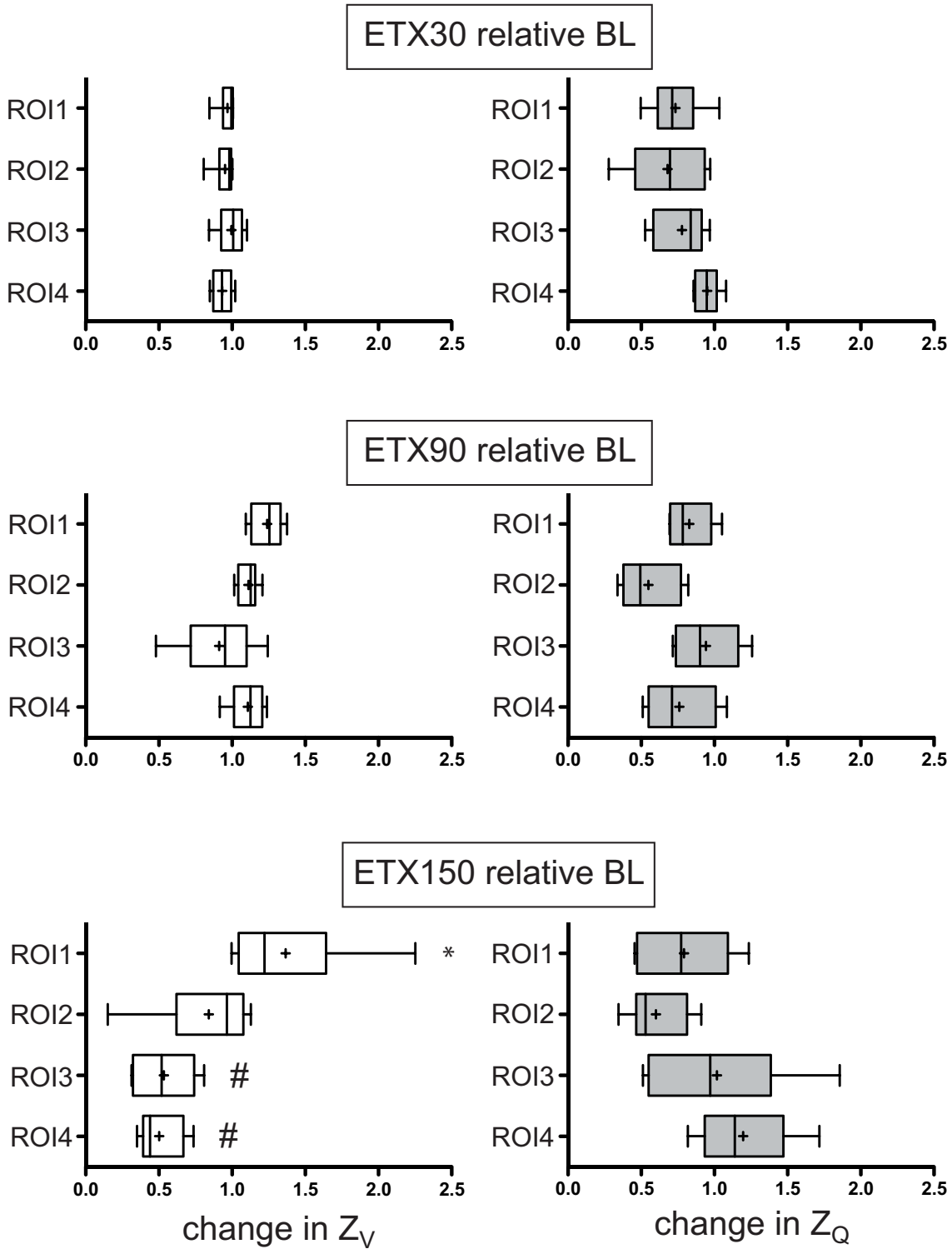

Figure 17. Fractional changes in Z_V or Z_Q during endotoxinaemia in CTRL animals. The fractional change in Z_V or Z_Q relative the BL value is illustrated in all ROIs following 30, 90 and 150 minutes of endotoxinaemia. Boxplots show the median, minimal-maximal value and the interquartile range. + denotes the mean value, * $p < 0.05$ increase vs. BL, # $p < 0.05$ decrease vs. BL.

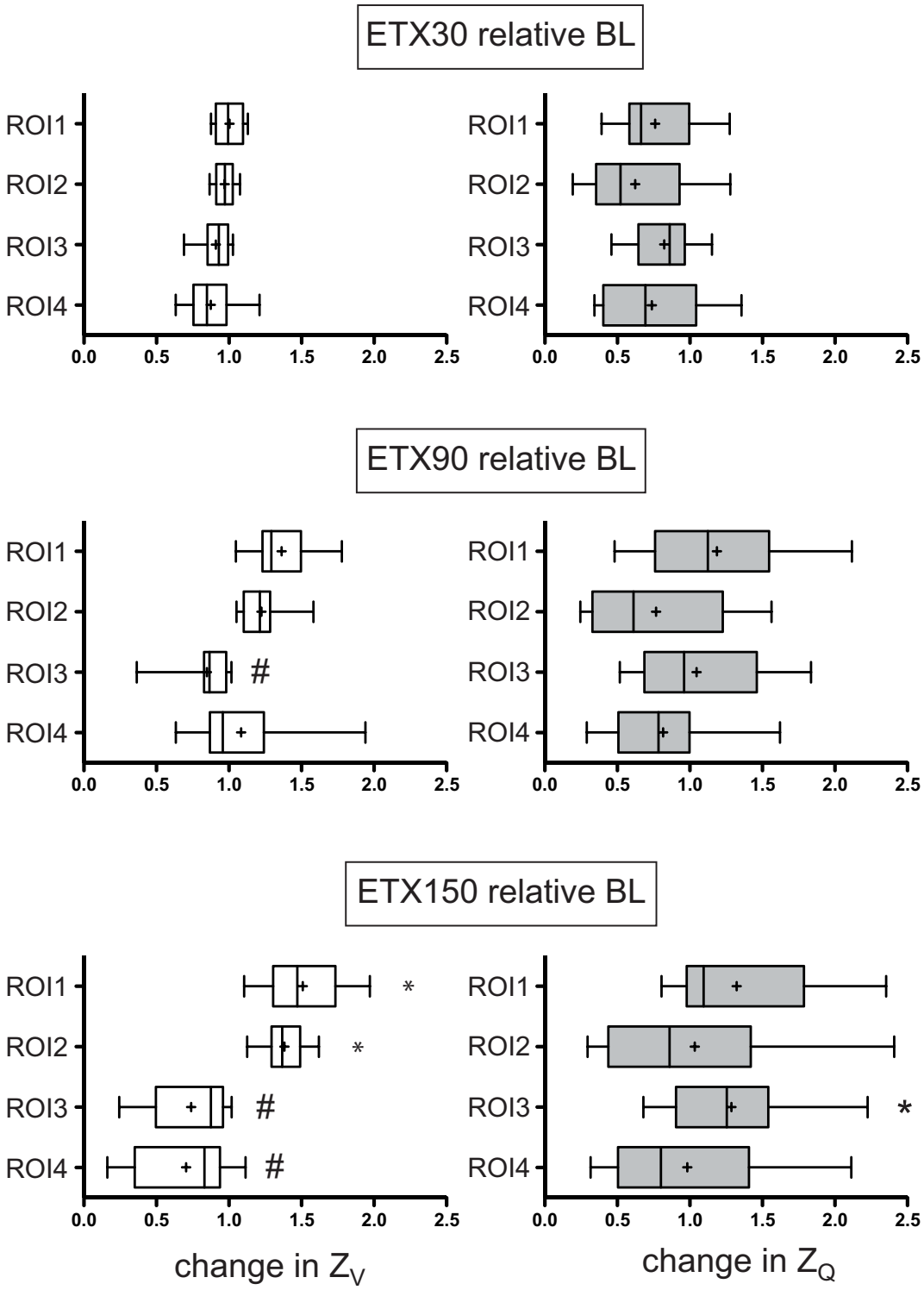

Figure 18. Fractional changes in Z_V or Z_Q during endotoxinaemia in ENAL animals. The fractional change in Z_V or Z_Q relative the BL value is illustrated in all ROIs following 30, 90 and 150 minutes of endotoxinaemia. Boxplots show the median, minimal-maximal value and the interquartile range. + denotes the mean value, * $p < 0.05$ increase vs. BL, # $p < 0.05$ decrease vs. BL.

DISCUSSION

The overall aim of this thesis was to evaluate the feasibility of EIT to assess pulmonary perfusion and its matching to ventilation. The monitoring of pulmonary ventilation by EIT has been investigated in several previous studies in relation to settings of mechanical ventilation, recruitment manoeuvres and the pathophysiology of acute lung injury. In contrast, few studies have assessed pulmonary perfusion and fewer still the matching of pulmonary ventilation and perfusion (V and Q). The V/Q matching is of fundamental importance in understanding and treating acute lung injury. The applicability of EIT to delineate V/Q relations could potentially advance treatment strategies.

A pig experimental model was used throughout all studies. First, the methodology to assess global perfusion was evaluated in the healthy state. Second, the methodology was expanded to include regional perfusion and its relation to ventilation. Third, the monitoring technique thus established was applied in pigs subjected to endotoxinaemic acute lung injury. Last, the efficacy of acute angiotensin-converting enzyme inhibition to ameliorate endotoxinaemic acute lung injury was investigated using the combined perfusion/ventilation monitoring strategy developed.

Global perfusion measurements

Perfusion related impedance changes may be assessed during ongoing ventilation or during apnoea. The study of perfusion during ventilation is the more physiological approach but perfusion measurements during a short apnoea hold important advantages. Pulse synchronous impedance changes are more readily discernible during apnoea and a stable baseline for measurements not existing in ventilation is achieved, substantially simplifying off-line calculations.
The impedance changes can be quantified in at least three distinct ways: measuring the amplitude of systolic impedance change, ΔZ_{sys}[15-17,20], plotting the impedance change as a function of time, measuring the amplitude of systolic impedance change (ΔZ_{sys}) together with the length of the impedance curve[18], or calculating the area under the impedance curve, AUC_Z.

The ΔZ_{sys} was used in this thesis to simplify programming of software for off-line analyses. To find maximal impedance amplitudes, 15-25 pulse beats were recorded during every apnoea. A sampling frequency of 10 Hz was chosen to optimise

signal-to-noise ratio. This frequency was four times or more than the maximal heart rate observed in any animal.
Each EIT curve demonstrated pulse-synchronous decreases in impedance corresponding to systole, and increases corresponding to diastole of the arterial pressure curve, providing enough precision to separate systolic and diastolic events, as reported previously[15]. Furthermore, the observation of a deflection in the impedance curve that corresponded to the dicrotic notch seen in the arterial pressure trace supported this notion.

To test an alternative method to quantify the impedance change, a test-series of AUC_Z calculations was made using data from study III. Pooling data on global EIT and corresponding SV obtained at baseline and during hyperdynamic endotoxinaemia resulted in a regression coefficient of 0.43 for AUC_Z compared to 0.47 for ΔZ_{sys}. Thus, similar, but not better, correlations to stroke volume were obtained using AUC_Z. It remains possible that an increased sampling frequency could have improved the accuracy of the impedance change integrals, AUC_Z.

Origin of the perfusion related impedance change

An important question raised in this thesis is whether the pulse synchronous impedance changes are related to an increase in pulmonary blood content or a decrease in pulmonary air content.
Three mechanisms may explain the relation between changes in thoracic impedance and the cardiac ejection of blood[102]. First, ventricular contraction causes a regional increase in impedance in the cardiac fossa during systole. Second, as erythrocytes align uniformly in the direction of the blood stream during systole, the negative charges on their surfaces cause a decrease in electrical impedance. During diastole the random spatial pattern of erythrocytes return and decrease the impact of the negative charge on the impedance of floating blood. Third, the stroke volume displaces the corresponding amount of air out of the lungs, resulting in a decrease in impedance following each systole.
The last mechanism is further supported by the large tidal volume and the high resistivity value of air compared to the stroke volume and blood (Table 1).
The compliance of the alveolus combined with the airway resistance limit how rapidly lungs fill with air, reducing the amount of air able to move into the alveolus during systole by approximately 30%[23]. The value 30% corresponds well to the underestimation of SV as assessed by EIT compared to measurements using the pulmonary artery catheter reported in study I.
The delayed increase in tracheal pressure following systole and the decrease in thoracic impedance could also be explained by the phase lag for pulmonary volume change. Recently, the amount of pulmonary blood flow, rather than the contact between heart and lungs, has been reported as the main determinant of the amplitude of cardiogenic oscillations of airway flow and pressure[111].

The question of whether changes in air or blood volume determine the pulse synchronous impedance change is still imperfectly understood and warrants further investigation. Possible methods to elucidate "the blood-air problem" could be to significantly enhance the conductivity of either air or blood. By injecting an impedance "contrast agent", for example a hypertonic saline solution[21,112] the perfusion signal can be enhanced by temporarily increasing the pulmonary vascular conductivity, registered by EIT as decreased impedance amplitudes.
Initial data from study I using a hypertonic saline bolus (RescueFlow, 3%) failed to generate reproducible impedance washout curves. In a so far unpublished report by Suarez-Sipman et al[113] a 5 ml bolus of NaCl 20% was used as a contrast agent, calculating the area over the injection curve as a measure of pulmonary perfusion.

Principles of separating ventilation and perfusion signals

Perfusion related impedance changes are normally observed superimposed on ventilatory changes. By holding the breath or by adding an inspiratory or expiratory pause to the ventilator, the perfusion related changes could be isolated. In this thesis, and end-expiratory pause was used to obtain an apnoeic period up to 20 seconds. While this approach facilitated considerably subsequent off-line analyses, it does not take into account circulatory-ventilatory interactions occurring during tidal ventilation.
Other investigators have used electrocardiogram-gated averaging of the impedance change[22,114], still not producing real-time images. Alternatively, frequency domain filtering has been applied[115,116], even if full separation of the ventilation and perfusion signals has not been attained. Recently, dynamic frequency filtering has been tested in a study on two healthy subjects resulting in a clear separation of ventilation and perfusion impedance signals superior to frequency domain filtering[21].

A fast Fourier transform (FFT) can be used to further study the frequency domains of ventilation and perfusion, generating a frequency spectrum of the EIT signal[117] that can be applied both for global and regional assessment. Two frequency bands are identified corresponding to the respiratory rate (and its second harmonic) and the heart rate.
A FFT was performed using pilot EIT data from this thesis. However, the temporal resolution of 10 Hz was not high enough for adequate separation. Using EIT data recorded with a frequency of 20 Hz obtained from a collaboration project, the FFT demonstrated the expected spectrum peaks corresponding to breathing and heart rate.

Accuracy of global perfusion measurements

The overall correlation coefficient of 0.62 for the amplitude of impedance change, ΔZ_{sys}, and stroke volume indicates that EIT provides a physiologically relevant estimate of pulmonary perfusion. In terms of assessing relative changes in pulmonary perfusion, the Bland-Altman analysis resulted in a bias of -7% with the 95% limits of agreement being − 51% to 36%. According to Critchley & Critchley[118] the limits of agreement between a new and the reference technique are acceptable up to ± 30%. Hence, the perfusion measurements as obtained by EIT in study I did not quite provide a clinically adequate measurement of stroke volume. However, a measurement error of 42% has been reported for thermodilution measurements of CO compared to ultrasonic flowmetry as the gold standard[119]. In view of this, the EIT technique could still be argued to perform favourably. It should be noted that the aim of study I was not to explore EIT as a monitor of SV but rather to establish the applicability of the technique to provide an estimate of pulmonary perfusion valid for comparisons to ventilation.

By inflating a balloon placed in the inferior caval vein, SV could be acutely reduced while leaving ventilation and pulmonary air volume unchanged. This intervention resulted in a good correlation between changes in ΔZ_{sys} and SV (ρ=0.73). The superior correlation of balloon-induced compared to PEEP-induced reduction of preload indicate that vascular distensibility is an important factor in determining the precision of perfusion measurements by EIT. Perfusion related impedance changes have been reported to be significantly smaller for the same SV in emphysematous patients with a reduced peripheral pulmonary vascular bed compared to controls[15], supporting the argument of a change in thoracic blood volume influencing the impedance change. Changes in blood flow velocity with no or minor changes in thoracic blood volume, might thus pass undetected by EIT. Notwithstanding, the volume calibrated ΔZ_{sys} signal demonstrated the best precision for low rather than high SVs in study I.

Limitations of EIT to detect perfusion changes

The functional or dynamic EIT approach to assess impedance change relative to a previously recorded baseline has some important features that need to be considered when analyzing and interpreting data.

Variable impedance properties as a consequence of significant changes in air volume (e.g. pneumothorax, emphysema, atelectases) or fluid volume (e.g. haemothorax, capillary leakage and formation of oedema) may confound the interpretation of the impedance amplitude relative the baseline. This may reduce accuracy if EIT imaging is considered entirely linear and impedance values interpreted in absolute terms over time[120].

The EIT algorithm used in the studies of this thesis generates a cross-sectional image of a mid-thoracic disc. The spatial resolution is highest close to the periphery and lowest in the central parts of the disc, possibly influencing image quality.
The currents injected accumulate impedance information from approximately five centimeters cranial and caudal to the level of the electrode belt[102], and some of the most cranial and caudal lung parts are therefore not assessed. This could to some extent explain the underestimation of stroke volume by EIT compared to thermodilution measurements using the pulmonary artery catheter as observed in study I.

To conclude, study I demonstrated that EIT could be used to monitor global pulmonary perfusion correlating to SV in both the resting state and during interventions resembling acute hypovolaemia and recruitment manoeuvres.

Regional perfusion measurements and the relation to ventilation

While study I evaluated EIT to monitor global perfusion, study II was designed to assess regional pulmonary perfusion distribution and the matching of V and Q by combined measurements of ventilation and perfusion. A second aim was to compare global EIT V/Q measurements to standard calculations of venous admixture and dead space.
The distribution of regional perfusion and V/Q measurements were evaluated at rest and during interventions designed to generate a wide range of V/Q ratios, similar to the interventions used in study I.

As discussed above, the changes in impedance related to perfusion (Z_Q) and ventilation (Z_V) differ by up to an order of magnitude. In an attempt to minimise this variability when comparing EIT measurements of ventilation and perfusion induced impedance changes, a common format of arbitrary units per minute (AU/min) was created by multiplying EIT amplitudes with respiratory and heart rate respectively.

Defining regions of interest (ROIs)

The software used for EIT analyses made studies of regional Z_Q and Z_V possible by the option of defining separate areas for impedance measurements, Regions Of Interest (ROIs).
Four ROIs were set along the ventrodorsal axis in each lung. A fixed height of each ROI (8 pixels) was by default set so that the four ROIs together would cover the full ventral to dorsal distance. Similarly, a fixed width (4 pixels) was used to

enclose the left or right lung areas. The only individualized adjustment made in each experiment was to set the medial borders of the ROIs outside the cardiac area. Individually positioned ROIs have the advantage of uniquely tailored settings but also the potential disadvantage of operator-related differences in setting the ROIs. Pilot data (not shown) indicated an increased inter- and intraobserver variability when ROIs were placed individually for each analysis.

Equally sized and positioned ROIs hold the advantage of being highly reproducible and operator independent. An alternative approach to define ROIs was performed by Hinz et al[35], using the mean impedance variation of the chest wall to set the boundary surrounding the lungs. Pulletz et al[121] defined the ROI contour as 20-35% of the maximum standard deviation of the pixel values.
The most dorsal ROI may involve areas with little lung tissue, as seen in ROI 4. This might be avoided by a tailored setting of the ROI. Such a potential error was evaluated by the Bland-Altman analysis made for ROIs extending the full EIT area measured compared to ROIs set to only enclose the pulmonary area of either the left or the right lung. The results demonstrated minor bias for all ROIs, including the most dorsal ROI 4.

The spatial resolution of EIT is, as described earlier, improving but still inferior to computed tomography and magnetic resonance imaging. The point spread function describes the response of an imaging system to a point source of for example impedance change. The degree of spreading, or blurring, of the point object is a measure of the quality of the imaging system. In the most dorsal ROI 4, the point spread function might blur the picture leading to a wider area interpreted as lung tissue. In ROI 1, the point spread function might lead to portions of the cardiac area being included in the recordings, despite defining the ROI to exclude the heart on the functional EIT image.

Regional perfusion and ventilation

The relative distribution of Z_V and Z_Q to each ROI was calculated as the proportion of the global, cumulative sum of ROI 1 to 4 for the left and right lung respectively. The greatest proportion of Z_Q and Z_V appeared in ROI 2 followed by approximately equal fractions in ROI 1 and 3. Furthermore, a largely parallel distribution of Z_V and Z_Q indicated a physiological V/Q ratio close to 1 at baseline. As would be expected, no significant differences were demonstrated between the left and right lungs.

An important finding in study II was the demonstration of acute regional changes in Z_Q following balloon inflation while ventilatory settings and thus Z_V were unchanged. The marked reduction of Z_Q in ROI 2 occurred with Z_Q maintained or even slightly increased in ROI 3 supported a redistribution of blood flow and not

merely an overall fall in pulmonary blood flow. A similar pattern of regionally divergent changes in Z_Q was observed following increased PEEP.

Significant correlations between global Z_V/Z_Q ratios and venous admixture and alveolar dead space supported the physiological relevance of the EIT measurements. This was further endorsed by the change in frequency distribution of Z_V/Z_Q ratios from the Gaussian-type at baseline to a markedly non-Gaussian pattern following interventions. The fact that even the global EIT measurements did not include the entire lung volume might explain why the correlation coefficients, while physiologically meaningful, did not indicate an absolute precision. Nevertheless, similar measurements during acute endotoxinaemia (study III), representing a model of severe V/Q mismatch, demonstrated significant and even stronger correlations.
The limitations in terms of spatial resolution and volume incorporated inherent to EIT measurements using a single electrode belt are likely to restrict precision similarly for any correlation to a global measurement, e.g. SV, Q_s/Q_t and V_d/V_t.
By calculating Z_V/Z_Q ratios within separate ROIs and at identical points in time, the confounding factor of an artifactual change in overall impedance relative the baseline was minimised.

Other methods to assess pulmonary perfusion and V/Q

No comparisons to other methods of assessing regional pulmonary perfusion or regional V/Q matching have been performed in this thesis. Global V/Q relations can be investigated using the multiple inert gas elimination technique (MIGET)[50]. Aerosolized and injected deposition of fluorescent labelled microspheres to measure regional ventilation and perfusion, was performed in an extensive study by Altemeier et al[45]. Instead of labelled microspheres, radionuclides may be inhaled and injected and traced three-dimensionally by positron emission tomography (PET)[29] or magnetic resonance imaging (MRI)[30,31]. Unfortunately, these methods have not been available to further evaluate the EIT measurements and derivations presented in this thesis.

To conclude, study II demonstrated that EIT could be used to monitor regional pulmonary perfusion and its relation to ventilation providing physiologically relevant estimates of V/Q matching.

Changes in regional Z_Q and Z_V during endotoxinaemic ALI

The EIT derived measures of pulmonary ventilation and perfusion evaluated in healthy lungs in studies I and II were implemented to study acute lung injury in

study III. The study was designed to focus on distribution and heterogeneity of Z_V and Z_Q following the induction of acute endotoxinaemia.

Endotoxinaemic ALI in pigs

Pigs are not humans, but share a similar physiology of pulmonary ventilation and perfusion[109,122]. The experimental endotoxinaemic condition contrasts from the critically ill septic patient in some important aspects. The pigs are young and otherwise healthy whereas the septic patient is commonly old and carries significant co-morbidities. The experimental protocol extended a few hours with acute endotoxinaemia, while the septic patient often presents with an unknown focus of infection, having been sick for several days.
The pig lungs contain pulmonary intravascular macrophages (PIMs), a population of mature macrophages adherent to endothelial cells in the capillaries. The presence of PIMs increases the acute susceptibility to lung injury following endotoxin infusion, compared to humans that lack PIMs[51].
Experimental endotoxinaemia is easily reproducible, is the second most common model of acute lung injury[51] and represents an established method to study early sepsis in our laboratory[123,124].

Heterogeneity of ventilation in endotoxinaemic ALI

In order to assess the distribution and heterogeneity of ventilation, measurements of respiratory mechanics were introduced. Apart from airway structure, posture, gravity and mode of ventilation, compliance and airway resistance influence alveolar filling rate and thereby the distribution of ventilation in physiological as well as pathological conditions.

Global volume dependant compliance (VDC), regional chord compliance and functional residual capacity (FRC) were assessed to evaluate some factors affecting distribution and heterogeneity of ventilation in endotoxinaemia.

Regional ventilation changes in endotoxinaemic ALI have been well studied, characterised by increased airway resistance and decreased pulmonary compliance[61], as also observed in this study.

Global VDC was progressively reduced in all portions of the tidal volume, most prominent in the high volume portion (VDC_{high}), consistent with gradual overdistension. Reduced global compliance developed as the result of formation of pulmonary oedema and pleural effusions, as clearly noticed when opening the pleural cavity to perform lung biopsies (study IV). Ascites formation is known to further comprise lung compliance and is commonly observed in the pig endotoxinaemic model used. However, by using transpulmonary pressure to

calculate VDC, the influence of chest wall compliance and abdominal pressure were excluded.

Regional chord compliance progressively deteriorated in all ROIs, notably in the dependent part of the lung. A ventral redistribution of ventilation was observed, in line with decreased regional compliance in ROI 3 and 4. Decreased dorsal compliance could relate to increased opening pressures in dependent lung areas as a result of pulmonary oedema.

The reduction in FRC correlated to the decreased global end-expiratory Z_V indicating decreased aerated lung volumes as endotoxinaemia proceeded.

Regional pulmonary filling characteristics, as outlined by Hinz et al[35], plots fractional regional tidal volumes versus global tidal volumes that is then analysed by polynomial regression.
A pilot analysis of regional pulmonary filling characteristics based on regional and global Z_V indicated alveolar recruitment in the dorsal regions, hyperinflation in ventral regions and a homogenous filling of alveoli in the mid-part of the lung at baseline. Following 150 minutes of endotoxinaemia similar but slightly more prominent filling characteristics were observed in ventral and dorsal lung parts whereas the mid-part exhibited alveolar recruitment. These results are in line with and support the changes in respiratory mechanics outlined above.

The relatively minor increase in Z_V heterogeneity observed over time when the datasets of regional Z_V were compared to the baseline are in line with previous reports by Gerbino et al[62].
The heterogeneity of ventilation, mainly oriented along the craniocaudal axis, with decreased compliance seen in areas adjacent to the diaphragm[28], might be underestimated by EIT measurements analysing Z_V in a transverse plane.

Heterogeneity of perfusion in endotoxinaemic ALI

The heterogeneity of pulmonary perfusion, as outlined in the introduction, is greater than for ventilation even in physiological conditions. The complex pattern of pulmonary perfusion is a particular challenge in endotoxinaemic ALI, as a result of atypical distribution of perfusion[60], pulmonary vasoconstriction[58] and impairment of hypoxic vasoconstriction.[59]

A dorsal redistribution of Z_Q was observed during acute endotoxinaemia. This result is in line with a previous report in endotoxinaemia of even shorter duration than that of this study. Furthermore, dorsal redistribution of perfusion has been suggested to occur independent of gravitational influence or oedema formation[60]. The impaired hypoxic vasoconstriction seen in endotoxinaemia could partly explain

the increased perfusion in dorsal regions despite the fact that ventilation was directed to ventral regions[59]. Other investigators have suggested that regional differences in the release and responsiveness to other vasoconstrictors such as thromboxane A_2 might explain the dorsal redistribution of perfusion in endotoxinaemia[62].

Similar to study I, global Z_Q correlated to SV. The superior correlation at baseline compared to late endotoxinaemia indicated an increase in heterogeneity of perfusion. This was further supported by the markedly decreased correlation observed when comparing the regional Z_Q datasets during progressive endotoxinaemia to the baseline.

In summary, pulmonary perfusion was more heterogeneous than ventilation already at baseline and this difference progressively increased during endotoxinaemia.

V/Q mismatch in endotoxinaemic ALI

Mismatch of ventilation and perfusion in endotoxinaemic ALI may be caused by increased heterogeneity of ventilation and/or perfusion, or ventilation and perfusion distributions changing in different magnitude and/or opposite directions.

The initial matching of global Z_V/Z_Q was close to perfect, as would be expected in healthy animals, but deteriorated during endotoxinaemia. Regional Z_V/Z_Q matching at baseline was consistent with dead space ventilation ventrally and venous admixture dorsally. The finding of a Z_V/Z_Q ratio consistent with dead space ventilation in ROI 1 in this study differs from the observations in study II, where the Z_V/Z_Q ratio in ROI 1 indicated venous admixture. This might represent a true variability between animals and experiments. Alternatively, the direct contribution of the heart to Z_Q in ROI 1 might have been reduced in study III compared to study II due to improved operator expertise in setting the ROI to exclude the cardiac area, which was also facilitated by the refined software used.

Endotoxinaemia induced a ventral redistribution of Z_V and a dorsal redistribution of Z_Q. The resulting Z_V/Z_Q mismatch was evident by impaired gas exchange demonstrated by progressive hypoxaemia and hypercapnia. Increased Z_V/Z_Q heterogeneity correlated to increased venous admixture, increased fractional alveolar dead space and increased alveolar–arterial difference. The heterogeneity of Z_Q was the predominant contributor to Z_V/Z_Q mismatch.

Endotoxinaemia induced persistent pulmonary hypertension in all animals and a hypotensive hyperdynamic state. Isolated pulmonary hyperperfusion in healthy animals is reported to increase V/Q mismatch[125], probably by elevating pulmonary artery pressure and extending intraregional heterogeneity.

The findings of reduced global Z_V/Z_Q ratio in this study correlates with the magnitude of reduced V/Q ratio found by Gerbino et al using aerosolized and injected microspheres for concurrent measurements of ventilation and perfusion as discussed above[60].

In the exudative phase of endotoxinaemic ALI, oedema evolves with consolidation and atelectases occurring predominantly in dependent lung regions[126]. The increased fluid content of the lungs might affect the EIT results as discussed previously, with functional impedance amplitudes decreasing as a result of increased tissue conductivity. While this may concern the regression analyses of Z_V and Z_Q heterogeneity, the redistributions of Z_V and Z_Q or the Z_V/Z_Q matching would not be affected though since these results are based on regional fractions of global impedance change, sharing a common timeline.

To conclude, study III demonstrated that EIT could be used to assess changes in regional ventilation and perfusion and matching of V/Q during endotoxinaemic ALI. Heterogeneity of ventilation and perfusion could also be evaluated using EIT to demonstrate the dynamics of V/Q relations during endotoxinaemic ALI.

Effects of enalapril on regional Z_Q and Z_V during endotoxinaemic ALI

Angiotensin II may contribute to the progression and non-resolution of ALI by multiple mechanisms including increased production of tumour necrosis factor-α and interleukins[93,94], increased endothelial adhesion and migration of inflammatory cells, apoptosis of endothelial[91] and alveolar epithelial cells[92], vasoconstriction and increased vascular permeability.
The relevance of Ang II mediated mechanisms in the early pathology of ALI has been demonstrated in previous experiments[127-129] using a similar protocol time frame as in this study. Changes occurring late in the pathology of ALI, such as collagen deposition and fibrogenesis, were beyond the scope of the protocol.

Increased ACE activity has been reported to correlate to worsened morbidity and mortality in ALI and ARDS, including a majority of patients with infectious pathogenesis.
This study was designed based on the hypothesis that early ACE inhibition, and thus reduced Ang II levels, would mitigate the pathophysiological pathways outlined above and thus attenuate V/Q mismatch and impaired gas-exchange in endotoxinaemic ALI. The EIT monitoring of V/Q heterogeneity and mismatch

established in study III was applied to evaluate the efficacy of enalapril administered prior to infusion of endotoxin.

Distribution and heterogeneity of ventilation and perfusion

Endotoxinaemia resulted in a dorsal redistribution of Z_Q and progessively increased heterogeneity of Z_Q. In contrast, a ventral redistribution was observed for Z_V with minor heterogeneity. Thus, the results were reproducible comparing studies III and IV. Similar changes were observed in enalapril pre-treated animals and in fact heterogeneity of Z_Q tended to be even further increased, although no statistical significance was attained.

The tendency to increased perfusion heterogeneity and a dorsal shift of perfusion, not matching ventilation, might be caused by impaired hypoxic vasoconstriction, possibly aggravated by enalapril. Blockade of Ang II receptor has been found to reduce pulmonary vascular tone in hypoxia[95,130], although disputed by other studies.[96,131]. Increased arterial hypoxaemia was not reported for Ang II receptor antagonists administered to subjects with chronic obstructive lung diease[132]. The effect of enalapril in study IV does not confirm the role for Ang II in hypoxic vasoconstriction since no statistically difference was observed.

The predominant heterogeneity of perfusion rather than ventilation during endotoxinaemia focuses interest on other potential vasoactive interventions. Interestingly, enalapril did not ameliorate the pulmonary hypertension associated with endotoxinaemia. Pulmonary hypertension induced by endotoxin is reported to be largely mediated by endothelin-induced venous constriction[133], endothelin being at least ten times as potent as Ang II[134]. This might explain the persistent pulmonary hypertension and the absent response to Ang II. Speculatively, the lack of vasodilation by AT_2 receptor agonism following enalapril might explain the earlier onset and higher pulmonary pressures observed in the treated group, even if not statistically different from control animals.

V/Q mismatch and gas exchange

Increased Z_V/Z_Q mismatch was observed overall and regionally in both control and enalapril-treated animals with no significant changes between groups. Consequently, similar changes between groups were observed for alveolar-arterial O_2 difference, venous admixture and fractional alveolar dead space. Again, equivalent effects of endotoxinaemia in studies III and IV support the reproducibility of the model.

The angiotensin II pathways

The effects of angiotensin II are principally mediated via two sets or receptors: AT_1 and AT_2, carrying different and to some extent reciprocal effects. The AT_1 receptor,

significantly and equally expressed both in control and enalapril-treated animals, has been reported to induce vascular permeability, vasoconstriction, inflammation and remodelling. Stimulation of the AT_2 receptor induces vasodilation. No expression of AT_2 was demonstrated in animals subjected to endotoxinaemic ALI. The lack of detectable AT_2 receptors might be explained by the relatively short protocol used in study IV, not permitting time enough for receptor up-regulation and surface expression[135]. Analytical issues seem less likely to explain the negative finding for AT_2 receptors, given that it has been demonstrated in earlier studies from our laboratory using the same method and animal species[136].
Convincing support for the pathway attributable to the deleterious effects of Ang II in ALI was thus provided by the Western Blot analyses. It remains possible that the lack of effect by enalapril pre-treatment was the results on inappropriate timing or dosing. Zhang et al reported[137] that tissue levels of Ang II were significantly elevated within three hours in a rodent model of endotoxinaemia. Cookson et al[129] demonstrated a significant increase in ACE in bronchoaleolar fluid of mice already at two hours following endotoxinaemia. Hence, it seems likely that the receptor, the agonist and the relevant enzyme necessary for enalapril to be effective would be present within the 150 minutes of the protocol used in study IV. The dose of enalapril has been used previously and shown to completely block the ACE mediated conversion of Ang I to Ang II even during severe hypovolemia[138].

Experimental studies have shown an attenuated inflammatory response[97,127] and increased survival[98] following selective AT_1 antagonism during acute endotoxinaemic ALI. It is thus possible that the negative result of study IV was related to the combined reduction of AT_1 and AT_2 agonism by enalapril, whereas a selective AT_1 antagonist may have produced other results, although no significant expression of AT_2 receptors was demonstrated in pigs. Species differences also need to be considered when comparing these results in murine and porcine models.

To conclude, study IV demonstrated reproducibility of the endotoxinaemic ALI model but failed to provide support for the hypothesis that ACE inhibition could attenuate alterations in the V/Q distribution and matching and thus improve gas exchange.

CONCLUSIONS

This thesis demonstrated the feasibility of EIT to monitor global pulmonary perfusion, correlating to a wide range of stroke volumes as measured by the pulmonary artery catheter, as well as regional pulmonary perfusion and its relation to ventilation providing physiologically relevant estimates of V/Q matching.

Global V/Q measurements significantly correlated to standard calculations of venous admixture and fractional alveolar dead space in the resting state and during interventions designed to resemble acute hypovolaemia and recruitment manoeuvres.

EIT could assess changes in regional ventilation and perfusion and V/Q matching during endotoxinaemic ALI.
The hypothesis that enalapril, by reducing levels of Ang II, could improve V/Q matching in endotoxinaemic ALI, was not supported by EIT measurements of V/Q matching nor by gas exchange variables.

In summary, EIT, by its relative ease of operation seems to be an interesting technique for ICU monitoring of distribution and matching of V and Q in the critically ill. The technique is still primarily a research tool and further investigations on pulmonary perfusion changes per se and the relation to ventilation are needed. The separation of ventilation and perfusion by new filter techniques is improving and needs further exploration. In a future perspective, the EIT technique warrants validation by other methods of assessing pulmonary perfusion both globally and regionally, for example MIGET and MRI or PET scans.

Clinical investigations are ongoing to assess pulmonary perfusion in pathological conditions commonly seen in the ICU.

ACKNOWLEDGEMENTS

I wish to express my sincere gratitude to

Prof **Anders Åneman,** tutor in science, colleague and friend. For being brilliant and true to your believes, for your never ending enthusiasm and bright sense of humour, for introducing me to the field of science and for excellent guiding, for introducing me to the world of Macs
Prof **Björn Biber**, Head of Dept of Anaesthesiology and Intensive Care, for your support and for giving me the opportunity to work on this thesis
Helén Seeman-Lodding, MD, PhD, former Head of Dept of Anaesthesia and Intensive Care, for giving me the opportunity to work on this thesis and for your belief in me
Johan Snygg, MD, PhD, Head of Dept of Anaesthesia and Intensive Care, for giving me the opportunity to work on this thesis
Søren Søndergaard, MD, PhD, co-author, for the most generous help and teaching, for your enthusiasm and great sense of humour
Prof **Ola Stenqvist**, co-author, for your support in initial studies and for sharing of expertise in pulmonary physiology
Sigurbergur Kárason, MD, PhD, co-author, for good advice and support, for setting such a high standard one how to write a book – your thesis
Anna Casselbrant, PhD, co-author, for good cooperation and sharing of expertise on the Western blot technique
All the staff at the Dept of Experimental Biomedicine, for the best assistance whenever needed
Eckardt Teckscher, Dräger Medical, Lübeck, for valuable and enthusiastic discussions on EIT
Robert Lorentsson, MTA, for valuable MATLAB help and solving problems on short notice
Lena Sandh, colleague and friend, for countless conversations and for being a true friend
Annette Nyberg, colleague and roommate, for generous support in all kinds of issues
Bertil Andersson, Anders Enskog, ICU colleagues and friends, for being the best of colleagues, for making me laugh
All colleagues in Dept of Anaesthesia and Intensive Care, for your encouragement and support throughout this thesis
Lisen, my sister and friend, for your never-ending support and friendship even when I do not keep in touch

My precious family, **Nicklas, Linn** and **Johan,** for all that matters

REFERENCES

1. Henderson RP, Webster JG: An impedance camera for spatially specific measurements of the thorax. IEEE Trans Biomed Eng 1978; 25: 250-4
2. Beck MS, Williams, R.: Process Tomography: Principles, Techniques and Applications, Butterworth-Heineman, 1995
3. Barber DC, Brown, B. H.: Applied potential tomography. J Phys Eng Sci Instrum 1984; 17: 723-33
4. Brown BH, Barber DC, Seagar AD: Applied potential tomography: possible clinical applications. Clin Phys Physiol Meas 1985; 6: 109-21
5. Holder DS: Electrical Impedance Tomography: Methods, History and Applications, Institute of Physics, 2004
6. Holder DS: Electrical impedance tomography (EIT) of brain function. Brain Topogr 1992; 5: 87-93
7. Frerichs I: Electrical impedance tomography (EIT) in applications related to lung and ventilation: a review of experimental and clinical activities. Physiol Meas 2000; 21: R1-21
8. Putensen C, Wrigge H, Zinserling J: Electrical impedance tomography guided ventilation therapy. Curr Opin Crit Care 2007; 13: 344-50
9. Victorino JA, Borges JB, Okamoto VN, Matos GF, Tucci MR, Caramez MP, Tanaka H, Sipmann FS, Santos DC, Barbas CS, Carvalho CR, Amato MB: Imbalances in regional lung ventilation: a validation study on electrical impedance tomography. Am J Respir Crit Care Med 2004; 169: 791-800
10. Meier T, Luepschen H, Karsten J, Leibecke T, Grossherr M, Gehring H, Leonhardt S: Assessment of regional lung recruitment and derecruitment during a PEEP trial based on electrical impedance tomography. Intensive Care Med 2008; 34: 543-550
11. Erlandsson K, Odenstedt H, Lundin S, Stenqvist O: Positive end-expiratory pressure optimization using electric impedance tomography in morbidly obese patients during laparoscopic gastric bypass surgery. Acta Anaesthesiol Scand 2006; 50: 833-9
12. Hinz J, Moerer O, Neumann P, Dudykevych T, Frerichs I, Hellige G, Quintel M: Regional pulmonary pressure volume curves in mechanically ventilated patients with acute respiratory failure measured by electrical impedance tomography. Acta Anaesthesiol Scand 2006; 50: 331-9
13. Meier T, Leibecke T, Eckmann C, Gosch UW, Grossherr M, Bruch HP, Gehring H, Leonhardt S: Electrical impedance tomography: changes in distribution of pulmonary ventilation during laparoscopic surgery in a porcine model. Langenbecks Arch Surg 2006; 391: 383-9

14. Luepschen H, Meier T, Grossherr M, Leibecke T, Karsten J, Leonhardt S: Protective ventilation using electrical impedance tomography. Physiol Meas 2007; 28: S247-60
15. Vonk Noordegraaf A, Kunst PW, Janse A, Marcus JT, Postmus PE, Faes TJ, de Vries PM: Pulmonary perfusion measured by means of electrical impedance tomography. Physiol Meas 1998; 19: 263-73
16. Smit HJ, Vonk Noordegraaf A, Roeleveld RJ, Bronzwaer JG, Postmus PE, de Vries PM, Boonstra A: Epoprostenol-induced pulmonary vasodilatation in patients with pulmonary hypertension measured by electrical impedance tomography. Physiol Meas 2002; 23: 237-43
17. Smit HJ, Vonk-Noordegraaf A, Marcus JT, van der Weijden S, Postmus PE, de Vries PM, Boonstra A: Pulmonary vascular responses to hypoxia and hyperoxia in healthy volunteers and COPD patients measured by electrical impedance tomography. Chest 2003; 123: 1803-9
18. Vonk-Noordegraaf A, 2nd, Janse A, Marcus JT, Bronzwaer JG, Postmust PE, Faes TJ, De Vries PM: Determination of stroke volume by means of electrical impedance tomography. Physiol Meas 2000; 21: 285-93
19. Smit HJ, Handoko ML, Vonk Noordegraaf A, Faes TJ, Postmus PE, de Vries PM, Boonstra A: Electrical impedance tomography to measure pulmonary perfusion: is the reproducibility high enough for clinical practice? Physiol Meas 2003; 24: 491-9
20. Smit HJ, Vonk Noordegraaf A, Marcus JT, Boonstra A, de Vries PM, Postmus PE: Determinants of pulmonary perfusion measured by electrical impedance tomography. Eur J Appl Physiol 2004; 92: 45-9
21. Deibele JM, Luepschen H, Leonhardt S: Dynamic separation of pulmonary and cardiac changes in electrical impedance tomography. Physiol Meas 2008; 29: S1-14
22. Kunst PW, Vonk Noordegraaf A, Hoekstra OS, Postmus PE, de Vries PM: Ventilation and perfusion imaging by electrical impedance tomography: a comparison with radionuclide scanning. Physiol Meas 1998; 19: 481-90
23. Lumb AB: Nunn´s Applied Respiratory Physiology, Sixth Edition, Butterworth-Heineman, 2005
24. Karason S, Karlsen KL, Lundin S, Stenqvist O: A simplified method for separate measurements of lung and chest wall mechanics in ventilator-treated patients. Acta Anaesthesiol Scand 1999; 43: 308-15
25. Navalesi P, Hernandez P, Laporta D, Landry JS, Maltais F, Navajas D, Gottfried SB: Influence of site of tracheal pressure measurement on in situ estimation of endotracheal tube resistance. J Appl Physiol 1994; 77: 2899-906
26. Karason S, Sondergaard S, Lundin S, Wiklund J, Stenqvist O: Evaluation of pressure/volume loops based on intratracheal pressure measurements during dynamic conditions. Acta Anaesthesiol Scand 2000; 44: 571-7
27. Karason S, Sondergaard S, Lundin S, Wiklund J, Stenqvist O: Direct tracheal airway pressure measurements are essential for safe and accurate dynamic

monitoring of respiratory mechanics. A laboratory study. Acta Anaesthesiol Scand 2001; 45: 173-9
28. Altemeier WA, McKinney S, Krueger M, Glenny RW: Effect of posture on regional gas exchange in pigs. J Appl Physiol 2004; 97: 2104-11
29. Harris RS, Schuster DP: Visualizing lung function with positron emission tomography. J Appl Physiol 2007; 102: 448-58
30. Kauczor HU, Chen XJ, van Beek EJ, Schreiber WG: Pulmonary ventilation imaged by magnetic resonance: at the doorstep of clinical application. Eur Respir J 2001; 17: 1008-23
31. Mills GH, Wild JM, Eberle B, Van Beek EJ: Functional magnetic resonance imaging of the lung. Br J Anaesth 2003; 91: 16-30
32. Mols G, Kessler V, Benzing A, Lichtwarck-Aschoff M, Geiger K, Guttmann J: Is pulmonary resistance constant, within the range of tidal volume ventilation, in patients with ARDS? Br J Anaesth 2001; 86: 176-82
33. Mols G, Brandes I, Kessler V, Lichtwarck-Aschoff M, Loop T, Geiger K, Guttmann J: Volume-dependent compliance in ARDS: proposal of a new diagnostic concept. Intensive Care Med 1999; 25: 1084-91
34. Karason S, Sondergaard S, Lundin S, Wiklund J, Stenqvist O: A new method for non-invasive, manoeuvre-free determination of "static" pressure-volume curves during dynamic/therapeutic mechanical ventilation. Acta Anaesthesiol Scand 2000; 44: 578-85
35. Hinz J, Gehoff A, Moerer O, Frerichs I, Hahn G, Hellige G, Quintel M: Regional filling characteristics of the lungs in mechanically ventilated patients with acute lung injury. Eur J Anaesthesiol 2007; 24: 414-24
36. Robertson HT, Glenny RW, Stanford D, McInnes LM, Luchtel DL, Covert D: High-resolution maps of regional ventilation utilizing inhaled fluorescent microspheres. J Appl Physiol 1997; 82: 943-53
37. Glenny RW, Lamm WJ, Albert RK, Robertson HT: Gravity is a minor determinant of pulmonary blood flow distribution. J Appl Physiol 1991; 71: 620-9
38. West JB, Dollery CT, Naimark A: Distribution of Blood Flow in Isolated Lung; Relation to Vascular and Alveolar Pressures. J Appl Physiol 1964; 19: 713-24
39. West JB: Blood Flow and Metabolism, Respiratory Physiology. The Essentials, Eighth Edition. Edited by Duffy N. Baltimore, Lippincott Williams & Wilkins, 2008
40. Hakim TS, Lisbona R, Dean GW: Gravity-independent inequality in pulmonary blood flow in humans. J Appl Physiol 1987; 63: 1114-21
41. Glenny RW, Robertson HT: Fractal properties of pulmonary blood flow: characterization of spatial heterogeneity. J Appl Physiol 1990; 69: 532-45
42. Brogan TV, Mellema JD, Martin LD, Krueger M, Redding GJ, Glenny RW: Spatial and temporal heterogeneity of regional pulmonary blood flow in piglets. Pediatr Res 2007; 62: 434-9

43. Glenny RW, Polissar NL, McKinney S, Robertson HT: Temporal heterogeneity of regional pulmonary perfusion is spatially clustered. J Appl Physiol 1995; 79: 986-1001
44. Galvin I, Drummond GB, Nirmalan M: Distribution of blood flow and ventilation in the lung: gravity is not the only factor. Br J Anaesth 2007; 98: 420-8
45. Altemeier WA, McKinney S, Glenny RW: Fractal nature of regional ventilation distribution. J Appl Physiol 2000; 88: 1551-7
46. Workman JM, Penman RW, Bromberger-Barnea B, Permutt S, Riley RL: Alveolar dead space, alveolar shunt, and transpulmonary pressure. J Appl Physiol 1965; 20: 816-24
47. de Waal EE, Wappler F, Buhre WF: Cardiac output monitoring. Curr Opin Anaesthesiol 2009; 22: 71-7
48. Pinsky MR: Hemodynamic evaluation and monitoring in the ICU. Chest 2007; 132: 2020-9
49. Wagner PD, Saltzman HA, West JB: Measurement of continuous distributions of ventilation-perfusion ratios: theory. J Appl Physiol 1974; 36: 588-99
50. Wagner PD: The multiple inert gas elimination technique (MIGET). Intensive Care Med 2008; 34: 994-1001
51. Matute-Bello G, Frevert CW, Martin TR: Animal models of acute lung injury. Am J Physiol Lung Cell Mol Physiol 2008; 295: L379-99
52. Ware LB, Matthay MA: The acute respiratory distress syndrome. N Engl J Med 2000; 342: 1334-49
53. Rubenfeld GD, Herridge MS: Epidemiology and outcomes of acute lung injury. Chest 2007; 131: 554-62
54. Luhr OR, Antonsen K, Karlsson M, Aardal S, Thorsteinsson A, Frostell CG, Bonde J: Incidence and mortality after acute respiratory failure and acute respiratory distress syndrome in Sweden, Denmark, and Iceland. The ARF Study Group. Am J Respir Crit Care Med 1999; 159: 1849-61
55. Cooke CR, Kahn JM, Caldwell E, Okamoto VN, Heckbert SR, Hudson LD, Rubenfeld GD: Predictors of hospital mortality in a population-based cohort of patients with acute lung injury. Crit Care Med 2008; 36: 1412-20
56. Brun-Buisson C, Minelli C, Bertolini G, Brazzi L, Pimentel J, Lewandowski K, Bion J, Romand JA, Villar J, Thorsteinsson A, Damas P, Armaganidis A, Lemaire F: Epidemiology and outcome of acute lung injury in European intensive care units. Results from the ALIVE study. Intensive Care Med 2004; 30: 51-61
57. Rubenfeld GD, Caldwell E, Peabody E, Weaver J, Martin DP, Neff M, Stern EJ, Hudson LD: Incidence and outcomes of acute lung injury. N Engl J Med 2005; 353: 1685-93
58. Lambermont B, Kolh P, Detry O, Gerard P, Marcelle R, D'Orio V: Analysis of endotoxin effects on the intact pulmonary circulation. Cardiovasc Res 1999; 41: 275-81

59. Weir EK, Mlczoch J, Reeves JT, Grover RF: Endotoxin and prevention of hypoxic pulmonary vasoconstriction. J Lab Clin Med 1976; 88: 975-83
60. Gerbino AJ, Altemeier WA, Schimmel C, Glenny RW: Endotoxemia increases relative perfusion to dorsal-caudal lung regions. J Appl Physiol 2001; 90: 1508-15
61. Dahm PL, Jonson B, De Robertis E, Myhre E, Svantesson C, Thorne J, Blomquist S: The effects of nitric oxide inhalation on respiratory mechanics and gas exchange during endotoxaemia in the pig. Acta Anaesthesiol Scand 1998; 42: 536-44
62. Gerbino AJ, McKinney S, Glenny RW: Correlation between ventilation and perfusion determines VA/Q heterogeneity in endotoxemia. J Appl Physiol 2000; 88: 1933-42
63. Huttemeier PC, Ringsted C, Eliasen K, Mogensen T: Ventilation-perfusion inequality during endotoxin-induced pulmonary vasoconstriction in conscious sheep: mechanisms of hypoxia. Clin Physiol 1988; 8: 351-8
64. Forsgren P, Jakobson S, Modig J: True shunt in relation to venous admixture in an experimental porcine model of early ARDS. Acta Anaesthesiol Scand 1989; 33: 621-8
65. Parsons PE, Worthen GS, Moore EE, Tate RM, Henson PM: The association of circulating endotoxin with the development of the adult respiratory distress syndrome. Am Rev Respir Dis 1989; 140: 294-301
66. Dantzker DR, Brook CJ, Dehart P, Lynch JP, Weg JG: Ventilation-perfusion distributions in the adult respiratory distress syndrome. Am Rev Respir Dis 1979; 120: 1039-52
67. Ralph DD, Robertson HT, Weaver LJ, Hlastala MP, Carrico CJ, Hudson LD: Distribution of ventilation and perfusion during positive end-expiratory pressure in the adult respiratory distress syndrome. Am Rev Respir Dis 1985; 131: 54-60
68. Levy MM, Fink MP, Marshall JC, Abraham E, Angus D, Cook D, Cohen J, Opal SM, Vincent JL, Ramsay G: 2001 SCCM/ESICM/ACCP/ATS/SIS International Sepsis Definitions Conference. Crit Care Med 2003; 31: 1250-6
69. Marshall JC, Reinhart K: Biomarkers of sepsis. Crit Care Med 2009; 29: 29
70. Angus DC, Linde-Zwirble WT, Lidicker J, Clermont G, Carcillo J, Pinsky MR: Epidemiology of severe sepsis in the United States: analysis of incidence, outcome, and associated costs of care. Crit Care Med 2001; 29: 1303-10
71. Vincent JL, Sakr Y, Sprung CL, Ranieri VM, Reinhart K, Gerlach H, Moreno R, Carlet J, Le Gall JR, Payen D: Sepsis in European intensive care units: results of the SOAP study. Crit Care Med 2006; 34: 344-53
72. Karlsson S, Varpula M, Ruokonen E, Pettila V, Parviainen I, Ala-Kokko TI, Kolho E, Rintala EM: Incidence, treatment, and outcome of severe sepsis in ICU-treated adults in Finland: the Finnsepsis study. Intensive Care Med 2007; 33: 435-43

73. Finfer S, Bellomo R, Lipman J, French C, Dobb G, Myburgh J: Adult-population incidence of severe sepsis in Australian and New Zealand intensive care units. Intensive Care Med 2004; 30: 589-96
74. Marshall RP, Gohlke P, Chambers RC, Howell DC, Bottoms SE, Unger T, McAnulty RJ, Laurent GJ: Angiotensin II and the fibroproliferative response to acute lung injury. Am J Physiol Lung Cell Mol Physiol 2004; 286: L156-64
75. Campbell DJ, Kladis A, Duncan AM: Nephrectomy, converting enzyme inhibition, and angiotensin peptides. Hypertension 1993; 22: 513-22
76. Maniatis NA, Orfanos SE: The endothelium in acute lung injury/acute respiratory distress syndrome. Curr Opin Crit Care 2008; 14: 22-30
77. Jerng JS, Hsu YC, Wu HD, Pan HZ, Wang HC, Shun CT, Yu CJ, Yang PC: Role of the renin-angiotensin system in ventilator-induced lung injury: an in vivo study in a rat model. Thorax 2007; 62: 527-35
78. Veerappan A, Reid AC, Estephan R, O'Connor N, Thadani-Mulero M, Salazar-Rodriguez M, Levi R, Silver RB: Mast cell renin and a local renin-angiotensin system in the airway: role in bronchoconstriction. Proc Natl Acad Sci U S A 2008; 105: 1315-20
79. Rigat B, Hubert C, Alhenc-Gelas F, Cambien F, Corvol P, Soubrier F: An insertion/deletion polymorphism in the angiotensin I-converting enzyme gene accounting for half the variance of serum enzyme levels. J Clin Invest 1990; 86: 1343-6
80. Ward WF, Molteni A, Ts'ao CH, Hinz JM: Captopril reduces collagen and mast cell accumulation in irradiated rat lung. Int J Radiat Oncol Biol Phys 1990; 19: 1405-9
81. Ortiz LA, Champion HC, Lasky JA, Gambelli F, Gozal E, Hoyle GW, Beasley MB, Hyman AL, Friedman M, Kadowitz PJ: Enalapril protects mice from pulmonary hypertension by inhibiting TNF-mediated activation of NF-kappaB and AP-1. Am J Physiol Lung Cell Mol Physiol 2002; 282: L1209-21
82. Wang R, Ibarra-Sunga O, Verlinski L, Pick R, Uhal BD: Abrogation of bleomycin-induced epithelial apoptosis and lung fibrosis by captopril or by a caspase inhibitor. Am J Physiol Lung Cell Mol Physiol 2000; 279: L143-51
83. Adamzik M, Frey U, Sixt S, Knemeyer L, Beiderlinden M, Peters J, Siffert W: ACE I/D but not AGT (-6)A/G polymorphism is a risk factor for mortality in ARDS. Eur Respir J 2007; 29: 482-8
84. Jerng JS, Yu CJ, Wang HC, Chen KY, Cheng SL, Yang PC: Polymorphism of the angiotensin-converting enzyme gene affects the outcome of acute respiratory distress syndrome. Crit Care Med 2006; 34: 1001-6
85. Marshall RP, Webb S, Bellingan GJ, Montgomery HE, Chaudhari B, McAnulty RJ, Humphries SE, Hill MR, Laurent GJ: Angiotensin converting enzyme insertion/deletion polymorphism is associated with susceptibility and outcome in acute respiratory distress syndrome. Am J Respir Crit Care Med 2002; 166: 646-50

86. Marshall RP, Webb S, Hill MR, Humphries SE, Laurent GJ: Genetic polymorphisms associated with susceptibility and outcome in ARDS. Chest 2002; 121: 68S-69S
87. Boldt J, Muller M, Heesen M, Harter K, Hempelmann G: Cardiorespiratory effects of continuous i.v. administration of the ACE inhibitor enalaprilat in the critically ill. Br J Clin Pharmacol 1995; 40: 415-22
88. Harding D, Baines PB, Brull D, Vassiliou V, Ellis I, Hart A, Thomson AP, Humphries SE, Montgomery HE: Severity of meningococcal disease in children and the angiotensin-converting enzyme insertion/deletion polymorphism. Am J Respir Crit Care Med 2002; 165: 1103-6
89. Villar J, Flores C, Perez-Mendez L, Maca-Meyer N, Espinosa E, Blanco J, Sanguesa R, Muriel A, Tejera P, Muros M, Slutsky AS: Angiotensin-converting enzyme insertion/deletion polymorphism is not associated with susceptibility and outcome in sepsis and acute respiratory distress syndrome. Intensive Care Med 2008; 34: 488-95
90. Lee JM, Lo AC, Yang SY, Tsau HS, Chen RJ, Lee YC: Association of angiotensin-converting enzyme insertion/deletion polymorphism with serum level and development of pulmonary complications following esophagectomy. Ann Surg 2005; 241: 659-65
91. Dimmeler S, Rippmann V, Weiland U, Haendeler J, Zeiher AM: Angiotensin II induces apoptosis of human endothelial cells. Protective effect of nitric oxide. Circ Res 1997; 81: 970-6
92. Ward WF, Molteni A, Ts'ao CH: Radiation-induced endothelial dysfunction and fibrosis in rat lung: modification by the angiotensin converting enzyme inhibitor CL242817. Radiat Res 1989; 117: 342-50
93. Ruiz-Ortega M, Lorenzo O, Suzuki Y, Ruperez M, Egido J: Proinflammatory actions of angiotensins. Curr Opin Nephrol Hypertens 2001; 10: 321-9
94. Suzuki Y, Ruiz-Ortega M, Lorenzo O, Ruperez M, Esteban V, Egido J: Inflammation and angiotensin II. Int J Biochem Cell Biol 2003; 35: 881-900
95. Morrell NW, Morris KG, Stenmark KR: Role of angiotensin-converting enzyme and angiotensin II in development of hypoxic pulmonary hypertension. Am J Physiol 1995; 269: H1186-94
96. Prewitt RL, Leffler CW: Feline hypoxic pulmonary vasoconstriction is not blocked by the angiotensin I-converting enzyme inhibitor, captopril. J Cardiovasc Pharmacol 1981; 3: 293-8
97. Liu L, Qiu HB, Yang Y, Wang L, Ding HM, Li HP: Losartan, an antagonist of AT1 receptor for angiotensin II, attenuates lipopolysaccharide-induced acute lung injury in rat. Arch Biochem Biophys 2009; 481: 131-6
98. Hagiwara S, Iwasaka H, Hidaka S, Hasegawa A, Koga H, Noguchi T: Antagonist of the type-1 ANG II receptor prevents against LPS-induced septic shock in rats. Intensive Care Med 2009; 35: 1471-8
99. Sondergaard S, Karason S, Wiklund J, Lundin S, Stenqvist O: Alveolar pressure monitoring: an evaluation in a lung model and in patients with acute lung injury. Intensive Care Med 2003; 29: 955-62

100. Baydur A, Behrakis PK, Zin WA, Jaeger M, Milic-Emili J: A simple method for assessing the validity of the esophageal balloon technique. Am Rev Respir Dis 1982; 126: 788-91
101. Olegard C, Sondergaard S, Houltz E, Lundin S, Stenqvist O: Estimation of functional residual capacity at the bedside using standard monitoring equipment: a modified nitrogen washout/washin technique requiring a small change of the inspired oxygen fraction. Anesth Analg 2005; 101: 206-12, table of contents
102. Bodenstein M, David M, Markstaller K: Principles of electrical impedance tomography and its clinical application. Crit Care Med 2009; 37: 713-24
103. Adler A, Amyot R, Guardo R, Bates JH, Berthiaume Y: Monitoring changes in lung air and liquid volumes with electrical impedance tomography. J Appl Physiol 1997; 83: 1762-7
104. Costa EL, Lima RG, Amato MB: Electrical impedance tomography. Curr Opin Crit Care 2009; 15: 18-24
105. Adler A, Guardo R, Berthiaume Y: Impedance imaging of lung ventilation: do we need to account for chest expansion? IEEE Trans Biomed Eng 1996; 43: 414-20
106. Bradford MM: A rapid and sensitive method for the quantitation of microgram quantities of protein utilizing the principle of protein-dye binding. Anal Biochem 1976; 72: 248-54
107. Hardman JG, Aitkenhead AR: Estimating alveolar dead space from the arterial to end-tidal CO(2) gradient: a modeling analysis. Anesth Analg 2003; 97: 1846-51
108. Bland JM, Altman DG: Calculating correlation coefficients with repeated observations: Part 1--Correlation within subjects. Bmj 1995; 310: 446
109. Dodds WJ, Abelseth MK: Criteria for selecting the animal to meet the research need. Lab Anim Sci 1980; 30: 460-5
110. Tumbleson ME: Swine in biomedical research. New York, Plenum press, 1987
111. Tusman G, Suarez-Sipmann F, Peces-Barba G, Climente C, Areta M, Arenas PG, Bohm SH: Pulmonary blood flow generates cardiogenic oscillations. Respir Physiol Neurobiol 2009; 167: 247-54
112. Frerichs I, Hinz J, Herrmann P, Weisser G, Hahn G, Quintel M, Hellige G: Regional lung perfusion as determined by electrical impedance tomography in comparison with electron beam CT imaging. IEEE Trans Med Imaging 2002; 21: 646-52
113. Suarez-Sipmann F: Titrating Open Lung PEEP in Acute Lung Injury, A clinical method based on changes in dynamic compliance, Department of Medical Sciences. Uppsala, Uppsala University, 2008
114. Eyuboglu BM, Brown BH, Barber DC: In vivo imaging of cardiac related impedance changes. IEEE Eng Med Biol Mag 1989; 8: 39-45
115. Leathard AD, Brown BH, Campbell J, Zhang F, Morice AH, Tayler D: A comparison of ventilatory and cardiac related changes in EIT images of

normal human lungs and of lungs with pulmonary emboli. Physiol Meas 1994; 15 Suppl 2a: A137-46
116. Zadehkoochak M, Blott BH, Hames TK, George RF: Pulmonary perfusion and ventricular ejection imaging by frequency domain filtering of EIT (electrical impedance tomography) images. Clin Phys Physiol Meas 1992; 13 Suppl A: 191-6
117. Frerichs I, Pulletz S, Elke G, Reifferscheid F, Schadler D, Scholz J, Weiler N: Assessment of changes in distribution of lung perfusion by electrical impedance tomography. Respiration 2009; 77: 282-91
118. Critchley LA, Critchley JA: A meta-analysis of studies using bias and precision statistics to compare cardiac output measurement techniques. J Clin Monit Comput 1999; 15: 85-91
119. Botero M, Kirby D, Lobato EB, Staples ED, Gravenstein N: Measurement of cardiac output before and after cardiopulmonary bypass: Comparison among aortic transit-time ultrasound, thermodilution, and noninvasive partial CO2 rebreathing. J Cardiothorac Vasc Anesth 2004; 18: 563-72
120. Hahn G, Just A, Dudykevych T, Frerichs I, Hinz J, Quintel M, Hellige G: Imaging pathologic pulmonary air and fluid accumulation by functional and absolute EIT. Physiol Meas 2006; 27: S187-98
121. Pulletz S, van Genderingen HR, Schmitz G, Zick G, Schadler D, Scholz J, Weiler N, Frerichs I: Comparison of different methods to define regions of interest for evaluation of regional lung ventilation by EIT. Physiol Meas 2006; 27: S115-27
122. Dodds WJ: The pig model for experimental research. Fed Proc 1982; 47: 247-8
123. Treggiari MM, Romand JA, Burgener D, Suter PM, Aneman A: Effect of increasing norepinephrine dosage on regional blood flow in a porcine model of endotoxin shock. Crit Care Med 2002; 30: 1334-9
124. Laesser M, Oi Y, Ewert S, Fandriks L, Aneman A: The angiotensin II receptor blocker candesartan improves survival and mesenteric perfusion in an acute porcine endotoxin model. Acta Anaesthesiol Scand 2004; 48: 198-204
125. Domino KB, Eisenstein BL, Tran T, Hlastala MP: Increased pulmonary perfusion worsens ventilation-perfusion matching. Anesthesiology 1993; 79: 817-26
126. Henzler D, Pelosi P, Dembinski R, Ullmann A, Mahnken AH, Rossaint R, Kuhlen R: Respiratory compliance but not gas exchange correlates with changes in lung aeration after a recruitment maneuver: an experimental study in pigs with saline lavage lung injury. Crit Care 2005; 9: R471-82
127. Hagiwara S, Iwasaka H, Matumoto S, Hidaka S, Noguchi T: Effects of an angiotensin-converting enzyme inhibitor on the inflammatory response in in vivo and in vitro models. Crit Care Med 2009; 37: 626-33
128. Yao S, Feng D, Wu Q, Li K, Wang L: Losartan attenuates ventilator-induced lung injury. J Surg Res 2008; 145: 25-32

129. Cookson WO, Wiseman MS, Shale DJ: Angiotensin converting enzyme and endotoxin induced lung damage in the mouse. Thorax 1985; 40: 774-7
130. Cargill RI, Lipworth BJ: Lisinopril attenuates acute hypoxic pulmonary vasoconstriction in humans. Chest 1996; 109: 424-9
131. Leeman M, Lejeune P, Naeije R: Inhibition of angiotensin-converting enzyme by perindopril diacid in canine oleic acid pulmonary edema. Crit Care Med 1987; 15: 567-73
132. Kiely DG, Cargill RI, Wheeldon NM, Coutie WJ, Lipworth BJ: Haemodynamic and endocrine effects of type 1 angiotensin II receptor blockade in patients with hypoxaemic cor pulmonale. Cardiovasc Res 1997; 33: 201-8
133. Rossi P, Persson B, Boels PJ, Arner A, Weitzberg E, Oldner A: Endotoxemic pulmonary hypertension is largely mediated by endothelin-induced venous constriction. Intensive Care Med 2008; 34: 873-80
134. Wanecek M, Weitzberg E, Rudehill A, Oldner A: The endothelin system in septic and endotoxin shock. Eur J Pharmacol 2000; 407: 1-15
135. Kaschina E, Unger T: Angiotensin AT1/AT2 receptors: regulation, signalling and function. Blood Press 2003; 12: 70-88
136. Ewert S, Laesser M, Johansson B, Holm M, Aneman A, Fandriks L: The angiotensin II receptor type 2 agonist CGP 42112A stimulates NO production in the porcine jejunal mucosa. BMC Pharmacol 2003; 3: 2
137. Zhang H, Sun GY: LPS induces permeability injury in lung microvascular endothelium via AT(1) receptor. Arch Biochem Biophys 2005; 441: 75-83
138. Aneman A, Pettersson A, Eisenhofer G, Friberg P, Holm M, von Bothmer C, Fandriks L: Sympathetic and renin-angiotensin activation during graded hypovolemia in pigs: impact on mesenteric perfusion and duodenal mucosal function. Shock 1997; 8: 378-84

POPULÄRVETENSKAPLIG SAMMANFATTNING

Lungornas ventilation och perfusion värderad med elektrisk impedanstomografi

Flödet av luft genom lungorna, ventilation, och flödet av blod, perfusion, och matchning av ventilation/perfusion är avgörande för gasutbytet i lungorna. Då blod och luft möts vid gränsen mellan alveol och lungkapillär sker ett utbyte av gaser, syrgas tillsätts till blodet och koldioxid lämnas för borttransport med utandningsluften. Det syrerika blodet lämnar lungorna för transport till kroppens samtliga organ.
Luft och blod matchas väl i friska lungor men ventilation/perfusions matchningen försämras ofta vid sjukdom eller påverkan på lungorna, vilket leder till sämre gasutbyte med dålig syrsättning och utvädring av koldioxid som följd.
Övervakning av ventilation och perfusion är därför centralt vid behandling av svåra sjukdomstillstånd.

Elektrisk impedanstomografi (EIT) är en icke-invasiv, icke strålande, kontinuerlig övervakningsteknik som med bilder beskriver impedansförändringar och dess fördelning i bröstkorgens olika vävnader. Impedans är det elektriska motståndet mot en växelström och mäts i Ω (ohm). Tekniken består av ett elektrodbälte omkring bröstkorgen där en svag ström skickas in genom ett elektrodpar och spänningsskillnaden som uppstår mäts i alla andra elektroder. Detta upprepas så att flera bilder kan sammanvägas till en slutlig tomografisk bild.
Bröstkorgens vävnader har olika elektriska egenskaper och därmed olika impedans, luft har ett högt elektriskt motstånd med hög impedans medan blod leder ström bra och har låg impedans. Dessa elektriska skillnader påverkar fördelningen av impedans i vävnaderna och typiska bilder för respektive ventilation och perfusion skapas.

Sepsis är ett tillstånd med allvarlig och spridd infektion och en vanlig orsak till intensivvård. Endotoxin är en del av bakteriers vägg som då det frisätts ger ett upphov till i stort sett samma förändringar som vid sepsis. För att efterlikna sepsis tillförs endotoxin i blodet.

Den här avhandlingen undersöker den elektriska impedanstomografi-teknikens möjligheter att värdera lungors perfusion och ventilation under friska förhållanden och vid endotoxin-utlöst akut lungskada i en experimentell gris-modell.
Global perfusion mättes med EIT under tillstånd med olika hjärtminutvolymer som mått på lunggenomblödning och jämfördes med standardmetoden för hjärtminutvolymmätning, pulmonalisartärkateter. EIT tekniken visade sig utföra mätningar väl jämförbara med standardmätningar.

Metoden utökades till att undersöka olika lungregioner var för sig, regionala perfusionsmätningar, och relationen till ventilation som ledde till skattningar av ventilations/perfusions förhållanden som var fysiologiskt relevanta. Globala EIT beräkningar av rubbningar i ventilations/perfusions förhållanden stämde väl överens med resultat från mätningar med standardmetoder av venös tillblandning (mer perfusion än ventilation) och det s.k. döda rummet (mer ventilation än perfusion).

Monitoreringstekniken har också använts till grisar med endotoxin-utlöst akut lungskada för att skatta förändringar i regional ventilation och perfusion. Ventilations/perfusions matchningen försämrades under endotoxin-tillförseln på grund av omfördelning av framför allt perfusion till de bakre lungdelarna samt en mer ojämn fördelning av perfusion över hela lungfälten.
Slutligen testades behandling med angiotensin-converting enzyme (ACE) hämmare (enalapril) för att minska nivåerna av angiotensin II, som kopplats till en ökad inflammatorisk aktivitet, och därmed förbättra ventilations/perfusions matchningen i den endotoxin-utlösta akuta lungskade modellen. Experimenten lyckades inte bekräfta hypotesen att ACE-hämmare skulle förbättra ventilations/perfusions matchningen och därmed gas utbytet vid endotoxin utlöst akut lungskada.

Sammanfattningsvis beskriver avhandlingen att elektrisk impedanstomografi kan användas för att uppskatta både global och regional lungperfusion samt relationen till ventilation under fysiologiska så väl som patologiska förhållanden.